



HAL
open science

Nickel(II) N-benzyl-N-methyldithiocarbamato complexes as precursors for the preparation of graphite oxidation accelerators

Zdenek Travnicek, Richard Pastorek, Pavel Starha, Igor Popa, Vaclav Slovak

► **To cite this version:**

Zdenek Travnicek, Richard Pastorek, Pavel Starha, Igor Popa, Vaclav Slovak. Nickel(II) N-benzyl-N-methyldithiocarbamato complexes as precursors for the preparation of graphite oxidation accelerators. *Journal of Inorganic and General Chemistry / Zeitschrift für anorganische und allgemeine Chemie*, 2010, 636 (8), pp.1557. 10.1002/zaac.201000091 . hal-00599864

HAL Id: hal-00599864

<https://hal.science/hal-00599864>

Submitted on 11 Jun 2011

HAL is a multi-disciplinary open access archive for the deposit and dissemination of scientific research documents, whether they are published or not. The documents may come from teaching and research institutions in France or abroad, or from public or private research centers.

L'archive ouverte pluridisciplinaire **HAL**, est destinée au dépôt et à la diffusion de documents scientifiques de niveau recherche, publiés ou non, émanant des établissements d'enseignement et de recherche français ou étrangers, des laboratoires publics ou privés.



**Nickel(II) N-benzyl-N-methyldithiocarbamato complexes as
 precursors for the preparation of graphite oxidation
 accelerators**

Journal:	<i>Zeitschrift für Anorganische und Allgemeine Chemie</i>
Manuscript ID:	zaac.201000091.R1
Wiley - Manuscript type:	Article
Date Submitted by the Author:	11-Mar-2010
Complete List of Authors:	Travnicek, Zdenek; Palacky University, Inorganic chemistry department Pastorek, Richard Starha, Pavel Popa, Igor Slovak, Vaclav
Keywords:	Nickel(II)complex, Dithiocarbamato ligand, Crystal structure, Graphite oxidation accelerator



ARTICLE

DOI: 10.1002/zaac.200


Nickel(II) *N*-benzyl-*N*-methyldithiocarbamate complexes as precursors for the preparation of graphite oxidation accelerators

Zdeněk Trávníček,^{*,[a]} Richard Pastorek,^[a] Pavel Štarha,^[a] Igor Popa,^[a] and Václav Slovák^[b]

Keywords: Nickel(II) complex; Dithiocarbamate ligand; Crystal structure; Graphite oxidation accelerator.

The nickel(II) *N*-benzyl-*N*-methyldithiocarbamate (BzMedtc) complexes [Ni(BzMedtc)(PPh₃)Cl] (**1**), [Ni(BzMedtc)(PPh₃)Br] (**2**), [Ni(BzMedtc)(PPh₃)I] (**3**) and [Ni(BzMedtc)(PPh₃)(NCS)] (**4**) were synthesized using the reaction of [Ni(BzMedtc)₂] and [NiX₂(PPh₃)₂], where X = Cl, Br, I and NCS. Subsequently, the complex **1** was used for the preparation of [Ni(BzMedtc)(PPh₃)₂]ClO₄ (**5**), [Ni(BzMedtc)(PPh₃)₂]BPh₄ (**6**) and [Ni(BzMedtc)(PPh₃)₂]PF₆ (**7**). The obtained complexes **1–7** were characterized by elemental analysis, thermal analysis and spectroscopic methods (IR, UV-Vis, ³¹P{¹H}-NMR). The results of the magnetochemical and molar conductivity measurements proved the complexes as diamagnetic non-electrolytes (**1–4**) or 1:1 electrolytes (**5–7**).

The molecular structures of **4** and **5**·H₂O were determined by a single crystal X-ray analysis. In all cases, the Ni(II) atom is four-coordinated in a distorted square-planar arrangement with the S₂PX, and S₂P₂ donor set, respectively. The catalytic influence of selected complexes **1**, **3**, **5**, and **6** on graphite oxidation was studied. The results clearly indicated that the presence of the products of thermal degradation processes of the mentioned complexes have impact on the course of graphite oxidation. A decrease in the oxidation start temperatures by about 60–100 °C was observed in the cases of all the tested complexes in comparison with pure graphite.

 * Corresponding Author

Fax: +420585 634 357

E-Mail: zdenek.travniczek@upol.cz

[a] Department of Inorganic Chemistry
Faculty of Science, Palacký University
Tr. 17. listopadu 12, CZ-771 46 Olomouc, Czech Republic

[b] Department of Chemistry
Faculty of Science, University of Ostrava
30. dubna 22, CZ-701 03 Ostrava, Czech Republic
Supporting information for this article is available on the
WWW under <http://dx.doi.org/10.1002/zaac.201000xxx> or
from the author.

Introduction

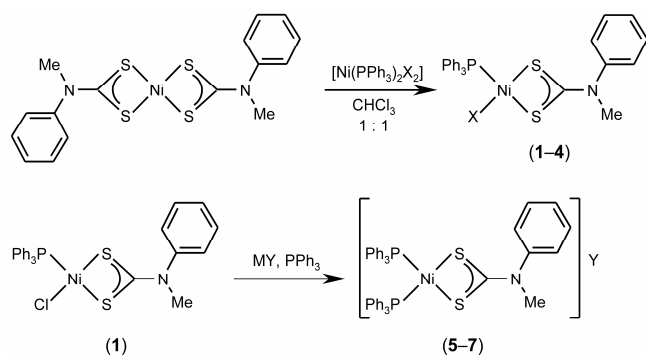
Many compounds involving the dithiocarbamate (dtc) moiety were reported up to now in connection with their applications. These compounds have been found to be useful as fungicides [1] or accelerators of vulcanization [2]. However, the spectrum of potential use of these compounds may be also broadened on the field of *in vitro* anticancer activity as can be demonstrated by the following examples. The 4(3*H*)-quinazolinone derivatives with dithiocarbamate side chains, such as (3,4-dihydro-2-methyl-4-oxoquinazolin-6-yl)-methyl-[4-(4-fluorophenyl)piperazine]-1-carbodithioate, showed promising *in vitro* anticancer activity (IC₅₀ = 0.5 μM) against human myelogenous leukaemia cell line (K562) [3]. Another dithiocarbamate derivative, 4-methylsulfinyl-1-(*S*-methyldithiocarbamyl)-butane (sulforamate), serves as a bearer of cancer chemopreventive effect [4]. The efficient protection of *N*-benzyl-*D*-glucamine-dithiocarbamate against cisplatin-induced nephrotoxicity (it is able to chelate platinum and thus to decrease the possibility of its reactions with sulphur-containing renal proteins or enzymes) has also been reported recently [5].

Several thousands of transition metal complexes involving the dithiocarbamate moiety have been prepared and reported to date and some of them are very promising from the biological activity point of view. The Pt(II) complex of the [Pt(esdt)(py)Cl] composition, where esdt = ethylsarcosinedithiocarbamate and py = pyridine, is highly cytotoxic against several human cancer cell lines, and moreover, this substance was not found as nephrotoxic, contrary to cisplatin [6]. [Au(dmdt)X₂] and [Au(esdt)X₂] are the representatives of non-platinum complex with the promising anticancer activity, which is even higher compared to cisplatin; dmdt = *N,N'*-dimethyldithiocarbamate, X = Cl or Br [7]. The antifungal activity, well-known for dithiocarbamate derivatives, was proved for tin(IV) complexes with pyrrolidine-dithiocarbamate [8].

Nickel is known as a suitable transition metal for the preparation of complexes and it is not surprising that over three thousand compounds (SciFinder, 2010) and 163 X-ray structures (Crystallographic Structural Database, CSD, ver. 5.30, September 2009 update [9]) involving a NiS₂CN motif have been reported to date. Among these compounds, the nickel(II) complexes involving the NiPN(S₂CN) or NiP₂(S₂CN) moiety, such as [Ni(4-MePzdtc)(PPh₃)(NCS)] [10], and [Ni(MeSdtc)(dppe)] [11], respectively, have been described in the literature; 4-MePzdtc = 4-methylpiperazine-dithiocarbamate anion, PPh₃ = triphenylphosphine, MeSdtc = *N*-methyl-*N*-sulfonyldithiocarbamate, dppe = 1,2-bis(diphenylphosphine)ethane. However, no nickel complexes containing the *N*-benzyl-*N*-methyldithiocarbamate anion (BzMedtc) within the mentioned moieties, have been reported to date.

The presented series of compounds follows a great number of nickel dithiocarbamate complexes previously prepared at our department [see ref. 12,13 and the references cited therein]. In this paper, we deal with seven nickel(II) complexes, whose structures, according to the literature research, for the first time involves a combination of the BzMedtc and PPh₃ ligands. The complexes [Ni(BzMedtc)(PPh₃)X] (**1–4**) were synthesized from [Ni(BzMedtc)₂], using its reaction with [NiX₂(PPh₃)₂], where X stands for Cl⁻ (for the complex **1**), Br⁻ (**2**), I⁻ (**3**) and NCS⁻ (**4**). The [Ni(BzMedtc)(PPh₃)₂]Y complexes (Y = ClO₄⁻ for **5**, BPh₄⁻ for **6** and PF₆⁻ for **7**) were prepared by the reaction of complex **1** with the appropriate alkaline salt and triphenylphosphine (see Scheme 1). The products were characterized by various physical methods including ³¹P{¹H}-NMR spectroscopy. The X-ray structures of the representatives of both types of complexes, i.e. [Ni(BzMedtc)(PPh₃)(NCS)] (**4**) and [Ni(BzMedtc)(PPh₃)₂]ClO₄·H₂O (**5**·H₂O), were determined by a single crystal X-ray analysis. The geometry of these compounds is square-planar with the NiS₂PN (**4**) and NiS₂P₂ (**5**·H₂O) donor sets.

This work also describes the effect of the nickel(II) dithiocarbamates on the oxidation of graphite as a model study of the coal combustion. As it is commonly known, the ignition temperature of the coal combustion is one of the most important properties influencing many industrial processes. This stage can be affected by the presence of both natural and artificial impurities [14,15]. Formerly, several papers reported simple nickel(II) compounds, such as NiO (mixed with KOH) or Ni(NO₃)₂ (mixed with K₂SO₄), as the substances accelerating graphite oxidation [16,17]. Few years ago, we decided to study the influence of the nickel(II, IV) dithiocarbamate complexes [see 13,18,19 and references cited therein] on the course of graphite oxidation. It was found that the presence of these complexes causes the ignition temperature decrease. Similar results were obtained also for the tested complexes **1**, **3**, **5**, and **6**, which were chosen as representatives of the presented compounds, as it is discussed in more detail within the framework of this paper.



Scheme 1. Schematic representation of the synthetic procedures applied for the preparation of the nickel(II) complexes **1–7**; X = Cl⁻ (**1**), Br⁻ (**2**), I⁻ (**3**) and NCS⁻ (**4**), MY = LiClO₄·3H₂O (**5**), Na[BPh₄] (**6**) and K[PF₆] (**7**).

Results and Discussion

The nickel(II) complexes **1–7** were prepared according to the synthetic strategies depicted in Scheme 1. The obtained molar conductivity values (Table 1) indicate that complexes **1–4** dissolved in acetone behave as non-electrolytes [20], which indirectly proved the coordination of the Cl⁻ (**1**), Br⁻ (**2**), I⁻ (**3**) and NCS⁻ (**4**) anions to the Ni(II) atom. On the other hand, the molar conductivity values of the remaining complexes proved the ionic nature (1:1 electrolyte type) in acetone (**5**) or DMF (**6**, **7**) solutions, which means that the ClO₄⁻ (**5**), BPh₄⁻ (**6**) and PF₆⁻ (**7**) anions are situated outside of the inner coordination sphere within the structure of the discussed complexes. The results of the room temperature magnetochemical measurements determined the prepared compounds to be diamagnetic, and thus, suggested on square-planar geometries in the vicinity of the central atom.

Table 1: The results of molar conductivity measurements, IR, UV-Vis and ³¹P{¹H}-NMR spectroscopy of the complexes **1–7**

λ_M^a	IR (cm ⁻¹) ^b			UV-Vis (cm ⁻¹) ^c	³¹ P{ ¹ H}-NMR δ^d (ppm)
	$\nu(C\equiv S)$	$\nu(C\equiv N)$	other		
1 2.2	990m	1510m		19 200	21.1s
				25 200	
				29 000	
2 2.1	996m	1520m		18 900	24.8s
				25 000	
				29 000	
3 9.3	998m	1520m		18 400	31.6s
				31 400	
4 1.7	996m	1528m	840m $\nu(C-S)$	20 400	22.8s
			2092s $\nu(C\equiv N)$	29 000	
5 99.0	996w	1542m	622m $\nu_4(ClO_4^-)$	19 900	32.0s
			1088s $\nu_3(ClO_4^-)$	31 000	
6 77.3	990m	1536s		20 700	32.1s
				30 900	
7 66.9	996m	1540m	836m $\nu_4(PF_6^-)$	19 800	32.0s,
				29 300	-143.6sp

[a] S cm² mol⁻¹ (10⁻³ M acetone solutions for **1–5** and 5 × 10⁻⁴ M DMF solutions for **6** and **7**); [b] KBr pellets (w = weak, m = middle, s = strong); [c] nujol technique; [d] CDCl₃ solutions (s = singlet, sp = septuplet)

Spectroscopic Characterization

The PPh₃ signals in the ³¹P{¹H}-NMR spectra of the CDCl₃ solutions of **1–7** were found in the range of 21.1–32.1 ppm (Table 1). These values differ significantly from that of -4.52 ppm determined for the free PPh₃ molecule, which is caused by electron density redistribution from phosphorus towards the Ni(II) centre as a consequence of PPh₃ coordination. The spectrum of **7** contains a septuplet at -143.6 ppm assignable to the PF₆⁻ anion. It should be noted that the chemical shift values of the complexes **1–4** increased in the order [Ni(Cl)(BzMedtc)(PPh₃)] (**1**) < [Ni(NCS)(BzMedtc)(PPh₃)] (**4**) < [Ni(Br)(BzMedtc)(PPh₃)] (**2**) < [Ni(I)(BzMedtc)(PPh₃)] (**3**), which agrees with the results reported for the nickel(II) complexes with *N*-benzyl-*N*-butyldithiocarbamate [12].

The maxima observed in the IR spectra of the nickel(II) complexes **1–7** at 990–998 cm⁻¹, and 1510–1542 cm⁻¹ (see Table 1) are typical for the $\nu(C\equiv S)$, and $\nu(C\equiv N)$ vibrations of the dithiocarbamate moiety, respectively [21,22]. The

peak of the $\nu(\text{C}=\text{S})$ stretching vibration is not split, which supports the bidentate coordination of the BzMedtc anion. The peaks of the $\nu(\text{C}\equiv\text{N})$ and $\nu(\text{C}-\text{S})$ vibrations of the NCS^- anion were observed in the IR spectrum of **4**. The ionic nature of the perchlorate anion in the complex **5**, can be supported by two undivided peaks at 622 and 1088 cm^{-1} [23]. The same conclusion can be made for the complex **7**, whose IR spectrum contains the non-split peak at 836 cm^{-1} assignable to $\nu(\text{PF}_6^-)$, which again indicates its ionic nature [24].

Table 2. Crystal data and structure refinements for $[\text{Ni}(\text{NCS})(\text{BzMedtc})(\text{PPh}_3)]$ (**4**) and $[\text{Ni}(\text{BzMedtc})(\text{PPh}_3)_2]\text{ClO}_4\cdot\text{H}_2\text{O}$ (**5**· H_2O)

Compound	4	5 · H_2O
Empirical formula	$\text{C}_{28}\text{H}_{25}\text{N}_2\text{NiPS}_3$	$\text{C}_{45}\text{H}_{42}\text{ClNNiO}_5\text{P}_2\text{S}_2$
Formula weight	575.36	897.02
Temperature (K)	113(2)	110(2)
Wavelength (\AA)	0.71073	0.71073
Crystal system	Monoclinic	Triclinic
Space group	$P2_1/n$	$P-1$
a (\AA)	13.6177(3)	11.47995(13)
b (\AA)	10.3556(2)	13.24049(16)
c (\AA)	19.1287(4)	15.02884(19)
α ($^\circ$)	90	70.3319(11)
β ($^\circ$)	92.4015(18)	84.5683(10)
γ ($^\circ$)	90	87.3995(9)
V (\AA^3)	2695.6(9)	2141.23(4)
Z , D_{calc} (g cm^{-3})	4, 1.418	2, 1.391
Absorption coefficient	1.032 mm^{-1}	0.734 mm^{-1}
Crystal size (mm)	0.30×0.25×0.25	0.40×0.35×0.30
F (000)	1192	932
θ range for data collection ($^\circ$)	$2.90 \leq \theta \leq 25.00$	$3.03 \leq \theta \leq 25.00$
Index ranges (h, k, l)	$-16 \leq h \leq 16$ $-9 \leq k \leq 12$ $-22 \leq l \leq 22$	$-13 \leq h \leq 13$ $-15 \leq k \leq 15$ $-17 \leq l \leq 15$
Reflections collected/unique	22656/4743	18531/7526
(R_{int})	(0.0246)	(0.0108)
Max./min. transmission	0.7825/0.7471	0.8099/0.7578
Data/restraints/parameters	4743/0/317	7526/0/553
Goodness-of-fit on F^2	1.065	1.039
Final R indices [$I > 2\sigma(I)$]	$R_1 = 0.0282$, $wR_2 = 0.0673$	$R_1 = 0.0342$, $wR_2 = 0.1009$
R indices (all data)	$R_1 = 0.0366$, $wR_2 = 0.0692$	$R_1 = 0.0388$, $wR_2 = 0.1031$
Largest peak/hole (e \AA^{-3})	0.344/−0.212	1.343 and −0.611

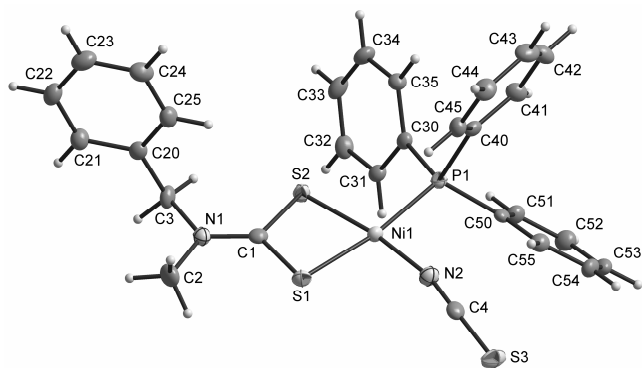


Figure 1. The molecular structure of $[\text{Ni}(\text{BzMedtc})(\text{PPh}_3)(\text{NCS})]$ complex (**4**) with non-hydrogen atoms drawn as thermal ellipsoids at the 50% probability level.

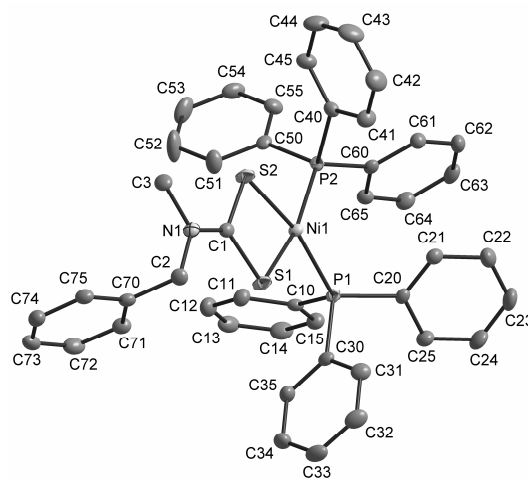


Figure 2. The molecular structure of $[\text{Ni}(\text{BzMedtc})(\text{PPh}_3)_2]\text{ClO}_4\cdot\text{H}_2\text{O}$ (**5**· H_2O) with non-hydrogen atoms drawn as thermal ellipsoids at the 50% probability level. The hydrogen atoms, perchlorate anion and water molecule of crystallization omitted for clarity.

Diffuse-reflectance electronic spectra of the prepared complexes **1–7** support the assumption of the square-planar geometry in the vicinity of the central Ni(II) atom. Absorption maxima at the 18 400–20 700 cm^{-1} region may be attributed to the $^1A_{1g} \rightarrow ^1B_{1g}$ transition of the square-planar nickel(II) complexes [25,26]. The next maxima, also assignable to the $d-d$ transitions, were found for the complexes **1** (25 200 cm^{-1}) and **2** (25 000 cm^{-1}). The maxima above 29 000 cm^{-1} are probably connected with the intraligand charge-transfer transitions in the S_2CN moiety [27].

X-ray Structure of $[\text{Ni}(\text{NCS})(\text{BzMedtc})(\text{PPh}_3)]$ (**4**) and $[\text{Ni}(\text{BzMedtc})(\text{PPh}_3)_2]\text{ClO}_4\cdot\text{H}_2\text{O}$ (**5**· H_2O)

The X-ray structure of the title complexes **4** (Figure 1) and **5**· H_2O (Figure 2) was determined by a single crystal X-ray analysis. The crystal data and structure refinements are given in Table 2, while the selected bond lengths and angles are summarized in Table 3.

The central Ni(II) ion of the complex **4** (Figure 1) is four-coordinated by PPh_3 , the isothiocyanate anion, and the bidentate-coordinated N -benzyl- N -methyldithiocarbamate anion (BzMedtc). The atoms of a NiS_2NP chromophore are arranged in the distorted square-planar geometry around the metal centre (Table 3). The Ni–S bond lengths of the title complex correlate well with the mean value of 2.204 \AA (2.155–2.258 \AA interval) determined for this band for the 116 square-planar nickel complexes involving bidentate-coordinated dithiocarbamate S-donor ligands, which have been up to now deposited in the Cambridge Structural Database (CSD) [9].

The well-known delocalization of π -electron density within the S_2CN moiety of the dithiocarbamate anion was observed for **4**, since the C–N and C–S bond lengths of the

studied compound (Table 2) were found to be significantly shorter compared to the single C–N (1.47 Å) and C–S (1.81 Å) σ -bond lengths [28]. Further, the C–S and C–N bond length values of BzMedtc are comparable with those of the transition metal (TM) complexes involving the (TM) S_2CNR_2 moiety and deposited within the CSD, which equal 1.717 Å, and 1.326 Å, respectively.

The S1 atom is the most deviated one [0.0454(5) Å] from the plane created through the Ni1, S1, S2, P1 and N2 atoms of the chromophore. Further, the described plane forms the dihedral angle of 83.10(5)° with the benzene ring of the BzMedtc molecule and dihedral angles of 67.90(5)°, 69.63(5)° and 47.85(4)° with the benzene rings of PPh₃ containing the C30, C40, and C50 atoms, respectively. Mutual orientation of the phenyl groups of PPh₃ within the molecular structure of **4** can be described by the 67.64(6)° (between benzene rings containing C30 and C40), 66.06(6)° (between benzene rings containing C30 and C50) and 76.53(6)° (between benzene rings containing C40 and C50) dihedral angles. The C–H...C, C–H...S and C...C types of the intramolecular non-bonding interactions were detected to stabilize the crystal structure of **4** (see Table 4). No typical hydrogen bond is present within the structure of discussed complex.

Table 3: Selected bond lengths (Å) and angles (°) for the complexes [Ni(NCS)(BzMedtc)(PPh₃)] (**4**) and [Ni(BzMedtc)(PPh₃)₂ClO₄·H₂O (**5**·H₂O)

Compound	4	5 ·H ₂ O
<i>Bond Lengths</i>		
Ni1–S1	2.2245(5)	2.2154(6)
Ni1–S2	2.1758(5)	2.2257(6)
Ni1–P1	2.2162(5)	2.2165(6)
Ni1–P2	-	2.2316(6)
Ni1–N2	1.8564(17)	-
C1–S1	1.7125(19)	1.731(2)
C1–S2	1.7214(19)	1.721(2)
C1–N1	1.306(2)	1.307(3)
N2–C4	1.163(2)	-
C4–S3	1.621(2)	-
<i>Bond Angles</i>		
S1–Ni1–S2	78.643(19)	78.29(2)
S1–Ni1–P1	171.63(2)	91.28(2)
S1–Ni1–N2	92.06(5)	-
S1–Ni1–P2	-	167.08(2)
S2–Ni1–P1	93.384(19)	167.76(2)
S2–Ni1–P2	-	88.91(2)
S2–Ni1–N2	170.70(5)	-
P1–Ni1–N2	95.91(5)	-
P1–Ni1–P2	-	101.24(2)
Ni1–S1–C1	85.71(7)	86.52(8)
Ni1–S2–C1	87.04(7)	86.42(8)
S1–C1–S2	108.60(11)	108.61(12)
S1–C1–N1	125.67(15)	126.50(17)
S2–C1–N1	125.73(15)	124.89(17)
Ni1–N2–C4	167.29(16)	-
N2–C4–S3	178.52(19)	-

In the case of **5**·H₂O, the Ni(II) ion is four-coordinated in the distorted square-planar geometry (Figure 2), similarly to the above described structure of complex **4**, by the bidentate-coordinated S-donor BzMedtc ligand and by two P-donor PPh₃ molecules. Selected bond lengths and angles

are given in Table 3. The positive charge of the [Ni(BzMedtc)(PPh₃)₂]⁺ cation is compensated by the perchlorate anion; the shortest Ni1...Cl1 distance equals 7.131(2) Å.

Table 4 Selected intramolecular non-bonding interactions and their parameters (Å, °) determined for the complexes **4** and **5**·H₂O

D–H...A	<i>d</i> (D–H)	<i>d</i> (H...A)	<i>d</i> (D...A)	<(DHA)
4				
C3–H3A...S3 ⁱ	0.990	2.9234(6)	3.666(2)	132.43(12)
C34–H34A...S2 ⁱⁱ	0.950	2.9389(5)	3.717(2)	139.90(12)
C32–H32A...S3 ⁱⁱⁱ	0.950	2.8695(6)	3.814(2)	172.48(12)
C31–H31A...S1 ⁱⁱⁱ	0.950	2.9701(6)	3.883(2)	161.56(12)
C2...C32			3.307(3)	
5 ·H ₂ O				
C74–H74A...C32 ^{iv}	0.950	2.771(3)	3.678(4)	160.13(16)
C72–H72A...C54 ^v	0.950	2.781(2)	3.554(3)	139.11(16)
C2–H2B...C74 ^{iv}	0.990	2.844(2)	3.771(3)	156.25(14)
C14–H14A...C33 ^{vi}	0.950	2.746(3)	3.666(4)	163.31(16)
C13–H13A...C3 ^v	0.950	2.879(2)	3.815(3)	168.16(14)
C44–H44A...C64 ^{vii}	0.950	2.872(3)	3.653(4)	140.17(16)
C13...C71 ^v			3.262(4)	
C70...C70 ^{iv}			3.391(3)	

Symmetry codes: (i) $x + 0.5, 0.5 - y, z - 0.5$; (ii) $1 - x, 1 - y, 1 - z$; (iii) $1.5 - x, y + 0.5, 1.5 - z$; (iv) $-x, -y, -z$; (v) $-x, 1 - y, -z$; (vi) $1 - x, 1 - y, -z$; (vii) $-x, 1 - y, 1 - z$

As it has been already mentioned in the case of complex **4**, the bond lengths within the NiS₂CN moiety of both structures show on electron density redistribution in connection with π -electron density delocalization (see the C–S and C–N bond lengths in Table 3). As for the Ni–P bonds of **5**, their lengths are in good agreement with the mean value of 2.208 Å (2.175–2.252 Å interval) as determined from 36 X-ray structures of tetra-coordinated nickel dithiocarbamate complexes involving at least one PPh₃ ligand and deposited within the CSD.

The S2 atom is the most deviated one [0.0903(6) Å] from the plane created through the atoms of the chromophore. The dihedral angles between this plane and benzene rings involving C10, C20, C30, C40, C50, C60, and C70 are 86.39(5)°, 58.49(7)°, 87.97(5)°, 70.52(5)°, 71.64(5)°, 63.60(6)°, and 71.98(5)°, respectively. Non-bonding interactions of the C–H...C and C...C types (C–H...O interactions with the distorted perchlorate anion and water molecule of crystallization are disregarded) were found in the crystal structure of the discussed nickel(II) complex (Table 4).

TG/DTA Thermal Analysis

The thermal properties of the prepared nickel(II) complexes were studied by TG and DTA methods. The TG and DTA curves of **1** and **6** are depicted in Figure 3. Although the chemical composition of these complexes is different, their thermal decomposition proceeded in a similar manner as indicated by analogical shapes of the TG curves. In cases of **2**, **3** and **6**, the sharp *exo*-effects with maxima at 188 °C, 193 °C, and 188 °C, respectively, were accompanied by mass increase on the TG curves, which can be attributed to the oxygen atom insertion into the Ni–P bond [29]. This effect was not registered on the TG curves of the remaining complexes, where the oxygen atom

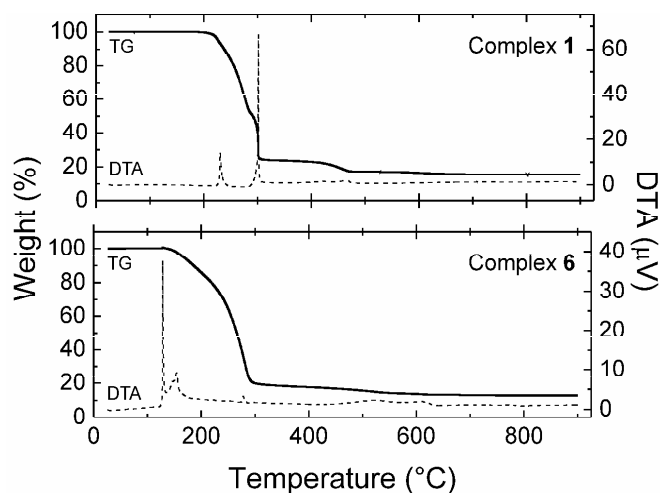


Figure 3. TG/DTA curves for complexes **1** and **6**.

insertion is most likely combined with the decomposition of the organic parts of the studied complexes.

The final products of the TG studies (900 °C) were studied by X-ray powder diffraction (XRD). NiO (PDF-4 No. 01-089-7130) was determined as the final product of the thermal decomposition of **1–4**. In the cases of the complexes **6** and **7**, the mixtures with significant predominance of NiO were detected. The final product of the TG thermal study of **6** also contains NiS (PDF-4 No. 4-004-5027) and Ni₃B₂O₆ (PDF-4 No. 4-008-3203), and some peaks could not be assigned. As for the complex **7**, Ni₂P₂O₇ (PDF-4 No. 01-074-1604) and Ni₃(PO₄)₂ (PDF-4 No. 01-072-3977) were detected by a XRD, while some peaks were not assigned.

Catalytic Influence of the Complexes on Graphite Oxidation

The influence of the presence of the representative complexes **1**, **3**, **5** and **6** on graphite oxidation were studied. The results, summarized in Figure 4 (obtained DTG curves) and Table 5 (obtained data), showed an positive influence on graphite oxidation, because the ignition temperature significantly decreased (by about 64–99 °C) after the addition of the tested nickel(II) complexes to a pure graphite.

Pure graphite oxidation proceeds in one step, while in the cases of its mixtures with the tested complexes, two steps in a larger temperature interval were detected on the appropriate DTG curves (Table 5). The first step takes place at lower temperature than pure graphite oxidation, whereas the oxidation rate maxima (T_m) of the second step approximately correspond to pure graphite. In addition, the oxidation mechanisms of both steps are different, as it can be seen from the activation energy (E) and frequency factor (A) values given in Table 5. More graphite was oxidized during the second step with higher E and A values.

At this point, we would like to discuss the described results of the influence on the graphite oxidation in connection with the results of TG/DTA studies. Figure 3 clearly shows that the thermal decomposition of the nickel(II) complexes is almost completely finished at the

temperature of ca. 700 °C and the weight loss above this temperature is insignificant. Based on this statement it may be concluded that not directly the discussed nickel(II) *N*-benzyl-*N*-methylthiocarbamato complexes, but the products of their thermal decomposition processes, affected graphite oxidation.

Table 5: Characteristic temperatures and kinetic parameters of catalytic influence on graphite given for pure graphite and its mixtures with nickel(II) complexes **1**, **3**, **5** and **6**

Sample	T (°C)	T_m (°C)	Step	n	A (s ⁻¹)	E	w (%)
Graphite	778–859	832		0.7	1.97×10^9	247	
1	679–838	792	I	1.3	3.62×10^7	190	43.58
			II	0.9	1.09×10^9	235	56.42
3	696–879	838	I	0.9	4.08×10^6	174	34.48
			II	0.9	9.10×10^7	220	65.52
5	693–860	815	I	1.0	1.47×10^7	183	36.06
			II	1.0	4.08×10^9	250	63.94
6	714–861	812	I	0.8	5.88×10^6	176	23.48
			II	1.1	1.17×10^9	238	76.52

T = temperature range of oxidation; T_m = oxidation rate maximum; n = reaction order; A = frequency factor; E = activation energy (kJ mol⁻¹); w = mass of sample oxidized

In connection with the above-mentioned facts, the tested complexes (except of **5**) were heated *in situ* to the temperatures corresponding to the beginning and end of graphite oxidation (see Table 5). The products of thermal decomposition relating to the mentioned temperatures were analysed by XRD. As for **1–4**, pure NiO was identified at both temperatures (Figure 5). The slight differences in the 2θ values were caused by a dilatation of the sample due to different measurement temperature. On the other hand, the mixtures of NiO, NiS and Ni₃B₂O₆ (for **6**) and Ni₂P₂O₇ and Ni₃(PO₄)₂ (for **7**) were detected by an XRD (Figure 5). Their quantitative composition was similar at both temperatures. Some peaks could not be assigned again.

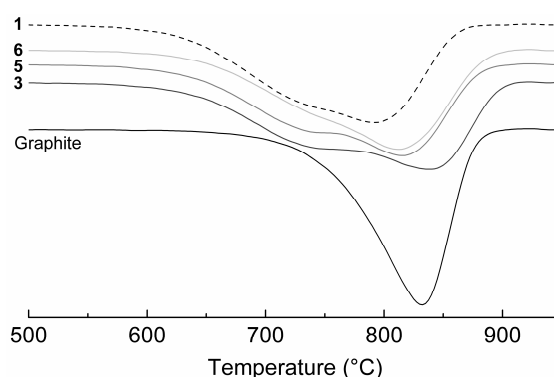


Figure 4. DTG curves obtained for pure graphite (black lines) and its mixture with the complexes **1** (black dashed lines), **3** (dark gray line), **5** (gray line) and **6** (light gray line); the tangent method was employed to determine the initial temperatures of the graphite oxidation

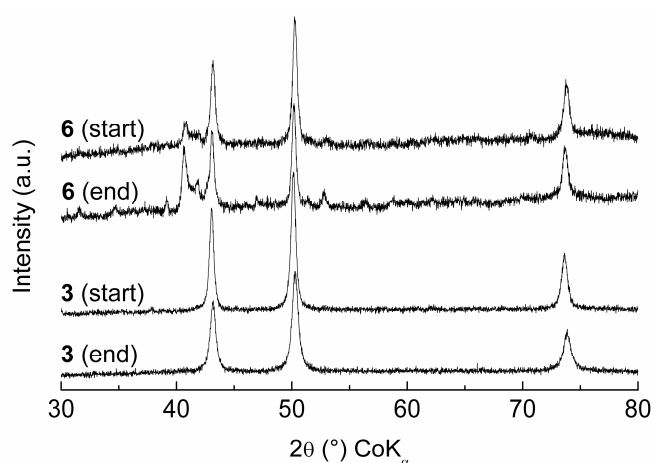


Figure 5. XRD patterns of the thermal decomposition products of the complexes **3** and **6**. The detected diffraction lines belong to NiO for **3**, and NiO, NiS and Ni₃B₂O₆ for **6**; the start and end temperatures are given in Table 5.

Conclusions

Seven nickel(II) complexes of the [Ni(BzMedtc)(PPh₃)X] (**1–4**) and [Ni(BzMedtc)(PPh₃)₂]Y (**5–7**) compositions were synthesized; X = Cl[−] for **1**, Br[−] for **2**, I[−] for **3** and NCS[−] for **4**, Y = ClO₄[−] for **5**, BPh₄[−] for **6** and PF₆[−] for **7**. The obtained powder products were fully characterized by elemental analysis, magnetochemical and molar conductivity measurements, thermal analysis and spectroscopic methods (IR, UV-Vis, ³¹P{¹H}-NMR). The molecular structures of the complexes [Ni(BzMedtc)(PPh₃)(NCS)] (**4**) and [Ni(BzMedtc)(PPh₃)₂]ClO₄·H₂O (**5**·H₂O) were determined by a single crystal X-ray analysis, which proved the distorted square-planar geometry with the bidentate-coordinated S-donor BzMedtc anion accompanied by PPh₃ and NCS[−] (**4**) or by two PPh₃ (**5**). This paper also describes the significant catalytic influence of the thermal degradation products of the selected complexes **1**, **3**, **5**, and **6** on graphite oxidation.

Experimental Section

Materials and General Methods

Chemicals and solvents were purchased from Sigma-Aldrich Co., Acros Organics Co., Lachema Co. and Fluka Co. and they were used as received. The starting compounds [Ni(BzMedtc)₂], [Ni(PPh₃)₂Cl₂], [Ni(PPh₃)₂Br₂], [Ni(PPh₃)₂I₂] and [Ni(PPh₃)₂(NCS)₂] were prepared according to the formerly reported synthetic pathways [13,30].

Elemental analyses (C, H, N) were performed on a Fisons EA-1108 CHNS-O Elemental Analyzer (Thermo Scientific). The content of nickel was determined using the chelatometric titration with murexide as an indicator. Chlorine, bromine and iodine contents were determined by the Schöniger method. Diffuse-reflectance spectra were recorded on a Perkin-Elmer Lambda35 UV/Vis spectrometer using a nujol technique. IR spectra (KBr pellets) were recorded on a Perkin-Elmer Spectrum one FT-IR spectrometer in the 450–4000 cm^{−1} region. The molar conductivity values of 10^{−3} M acetone solutions of **1–5** and 5 × 10^{−4} M

N,N'-dimethylformamide (DMF) solutions of **6** and **7** were determined by an LF 330/SET conductometer (WTW GmbH) at 25 °C. The room temperature magnetic susceptibilities were measured using the Faraday method with a laboratory designed instrument with a Sartorius 4434 MP-8 microbalance; Co[Hg(NCS)₄] was used as a calibrant and the correction for diamagnetism was performed using Pascal constants. Simultaneous thermogravimetric (TG) and differential thermal (DTA) analyses were performed by an Exstar TG/DTA 6200 (Seiko Instruments Inc.) in a platinum crucible and dynamic air atmosphere (100 mL min^{−1}) from the laboratory temperature to 1050 °C with a 2.5 °C min^{−1} temperature gradient. The weights of the studied complexes **1–4**, **6** and **7** (**5** was not studied for safety reasons, since it contains the perchlorate anion) were ca. 10 mg. ³¹P{¹H}-NMR spectra of the CDCl₃ solutions were measured on a Bruker Avance 300 spectrometer at 300 K and the spectra were calibrated against 85% H₃PO₄ used as an external reference. X-ray powder diffraction experiments were performed with a PANalytical X'Pert PRO instrument (Co-Kα radiation) equipped with an X'Celerator detector. Samples were placed on a zero-background Si slide and scanned in the 2θ range of 5–90° in the steps of 0.017°. *In situ* measurements were realized in the reaction cell XRK900 (Anton Paar). Evaluation was made using HighScore Plus software and PDF-4 database.

Single Crystal X-ray Analysis of the Complexes **4** and **5**·H₂O

A single crystal X-ray measurement was performed on an Xcalibur™2 diffractometer (Oxford Diffraction Ltd.) with Sapphire2 CCD detector, and with Mo Kα (Monochromator Enhance, Oxford Diffraction Ltd.) and at 113 K (**4**) and 110 K (**5**·H₂O). Data collection and reduction were performed by a CrysAlis software [CrysAlis CCD and CrysAlis RED, Version 1.171.33.52, Oxford Diffraction Ltd., Abingdon, England, 2009]. The same software was used for data correction for an absorption effect by the empirical absorption correction using spherical harmonics, implemented in SCALE3 ABSPACK scaling algorithm. Both structures were solved by direct methods using SHELXS-97 software [31] and refined on *F*² using the full-matrix least-squares procedure (SHELXL-97). Non-hydrogen atoms were refined anisotropically and all hydrogen atoms were located in difference Fourier maps and refined by using the riding model with C–H = 0.95, 0.98 and 0.99 Å, and *U*_{iso}(H) = 1.2*U*_{eq}(CH, CH₂) or 1.5*U*_{eq}(CH₃), except for those belonging to the crystal water molecule in **5**. The perchlorate anion as well as crystal water molecule was refined as disordered over two positions with the occupancy factors 75% and 25%, and 57% and 43%, respectively. The crystal data and structure refinements of **4** and **5** are given in Table 1. The molecular graphics were drawn and the additional structural calculations were interpreted using DIAMOND [32]. Crystallographic data have been deposited with the Cambridge Crystallographic Data Centre, 12 Union Road, Cambridge CB21EZ, UK (Fax: +44-1223-336033; E-Mail: deposit@ccdc.cam.ac.uk). Copies of the data can be obtained free of charge on application to CCDC, as the depository numbers CCDC-766048 (**4**) and CCDC-766049 (**5**·H₂O).

The Catalytic Study

Graphite (0.6 g, diameter of particles less than 0.1 mm, ash residue max. 0.2%, mass drying loss max. 0.2%) was mixed with an

acetone solution (2 mL) of the nickel(II) complex **1**, **3**, **5** or **6** (**2**, **4**, and **7** were not studied because of their insufficient solubility in acetone) to give the final nickel concentration of 2.5 mmol L⁻¹. The mixtures were homogenized and dried at room temperature for 24 h. The study of the catalytic influence of these samples on graphite was performed on a Netzsch STA 449C device with an α -Al₂O₃ crucible without a standard (10 °C min⁻¹ heating rate, sample weight of 5.0 mg, 100 mL min⁻¹ dynamic air atmosphere). The intersection point of the DTG curve tangents represents the initial temperatures of the graphite oxidation. The kinetic parameters were calculated by a direct non-linear regression method [33].

Syntheses of the Nickel(II) Complexes 1–7

[Ni(BzMedtc)(PPh₃)Cl] (1), **[Ni(BzMedtc)(PPh₃)Br] (2)**, **[Ni(BzMedtc)(PPh₃)] (3)** and **[Ni(BzMedtc)(PPh₃)(NCS)] (4)**: The complex **1** was synthesized using the reaction of [Ni(BzMedtc)₂] (1 mmol) and [NiCl₂(PPh₃)₂] (1 mmol). Both starting compounds were suspended in 25 mL of chloroform (CHCl₃). The mixture was stirred at room temperature until the reaction components were completely dissolved. The resulting solution was filtered through activated carbon. Diethyl ether was added to the filtrate which was left to stand at laboratory temperature. The precipitate of **1** formed in a few days. The product was filtered off, washed with diethyl ether and dried at 40 °C under an infrared lamp. The complexes **2–4** were prepared as described for **1**, but [NiBr₂(PPh₃)₂] (for **2**), [NiI₂(PPh₃)₂] (for **3**) and [Ni(NCS)₂(PPh₃)₂] (for **4**) were used instead of [NiCl₂(PPh₃)₂]. In the case of the complex **4**, the crystals suitable for a single crystal X-ray analysis were obtained from the mother liquor in two days. **[Ni(BzMedtc)(PPh₃)Cl] (1)**: Yield: 78%. Colour: violet. C₂₇H₂₅NS₂PClNi (M_r = 552.8); C 58.7 (calc. 58.4); H 4.6 (4.6); N 2.5 (2.4); S 11.6 (11.3); Cl 6.4 (6.5); Ni 10.6 (10.6)%. **[Ni(BzMedtc)(PPh₃)Br] (2)**: Yield: 90%. Colour: violet. C₂₇H₂₅NS₂PBrNi (M_r = 597.2); C 54.3 (calc. 54.2); H 4.2 (4.1); N 2.3 (2.0); S 10.7 (10.3); Br 13.4 (13.1); Ni 9.8 (9.6)%. **[Ni(BzMedtc)(PPh₃)] (3)**: Yield: 70%. Colour: dark violet. C₂₇H₂₅NS₂PINi (M_r = 644.2); C 50.3 (calc. 49.9); H 3.9 (3.9); N 2.2 (2.2); S 10.0 (10.0); I 19.7 (19.3); Ni 9.1 (9.2)%. **[Ni(BzMedtc)(PPh₃)(NCS)] (4)**: Yield: 82%. Colour: red. C₂₈H₂₅N₂S₃PNi (M_r = 575.4); C 58.5 (calc. 58.9); H 4.4 (4.1); N 4.9 (4.7); S 16.7 (16.6); Ni 10.2 (10.3)%. **[Ni(BzMedtc)(PPh₃)₂]ClO₄ (5)**: LiClO₄·3H₂O (2 mmol) was poured to a suspension of the complex **1** (1 mmol) and PPh₃ (2 mmol) in methanol (25 mL). The reaction mixtures were refluxed for 3 h. The resulting solution was filtered through activated carbon and left to stand at room temperature. The crystals of **5**·H₂O suitable for a single crystal X-ray analysis formed from the mother liquor in a few days. The complex was filtered off, washed with methanol and diethyl ether and dried at 40 °C under an infrared lamp. Yield: 47%. Colour: pink. C₄₅H₄₀NS₂P₂ClO₄Ni (M_r = 879.0); C 61.5 (calc. 61.8); H 4.6 (4.3); N 1.6 (1.5); S 7.3 (6.9); Cl 4.2 (4.6); Ni 6.7 (6.8)%. **[Ni(BzMedtc)(PPh₃)₂]BPh₄ (6)**: 2 mmol of Na[BPh₄] was added to a suspension of **1** (1 mmol) and PPh₃ (2 mmol) in 25 mL of methanol. The pink solid appeared during 3 h of the reaction mixture refluxing. The product was removed by filtration, washed (methanol and diethyl ether) and dried at 40 °C under an infrared lamp. Yield: 69%. Colour: pink. C₆₉H₆₀NS₂P₂BNi (M_r = 1098.8); C 75.4 (calc. 75.1); H 5.5 (5.2); N 1.3 (1.5); S 5.8 (5.6); Ni 5.3 (5.7)%.

[Ni(BzMedtc)(PPh₃)₂]PF₆ (7): The solutions of PPh₃ (2 mmol; 5 mL of acetone) and K[PF₆] (1 mmol; 7 mL of acetone) were separately added to a solution of **1** (1 mmol; 5 mL of chloroform). The reaction mixture was refluxed for a period of 4 h and after that it was filtered through activated carbon. Diethyl ether was added to the filtrate, which caused the formation of the precipitate. The solid was filtered off, washed with diethyl ether and dried at 40 °C under an infrared lamp. Yield: 54%. Colour: red. C₄₅H₄₀NS₂P₃F₆Ni (M_r = 924.5); C 58.5 (calc. 58.8); H 4.4 (4.6); N 1.6 (1.9); S 6.9 (6.5); Ni 6.3 (6.7)%.

Acknowledgement

This work was financially supported by The Ministry of Education, Youth and Sports of the Czech Republic (a grant no. MSM6198959218). The authors also thank Assoc. Prof. Zdeněk Šindelář for magnetic susceptibility measurements, Dr. Jan Filip for X-Ray powder diffraction experiments.

References

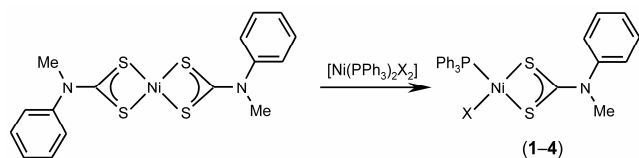
- [1] G. Hogarth, *Prog. Inorg. Chem.* **2005**, *53*, 71–561
- [2] P. J. Nieuwenhuizen, A. W. Ehlers, J. G. Haasnoot, S. R. Janse, J. Reedijk, E. J. Baerends, *J. Am. Chem. Soc.* **1999**, *121*, 163–168
- [3] S. L. Cao, Y. P. Feng, Y. Y. Jiang, S. Y. Liu, G. Y. Ding, R. T. Li, *Bioorg. Med. Chem.* **2005**, *15*, 1915–1917
- [4] C. Gerhauser, M. You, J. Liu, R. M. Moriarty, M. Hawthorne, R. G. Metha, R. C. Moon, J. M. Pezzuto, *Cancer Res.* **1997**, *57*, 272–278
- [5] S. Hidaka, T. Funakoshi, H. Shimada, M. Tsuruoka, S. Kojima, *J. App. Toxicol.* **1995**, *15*, 167–273
- [6] C. Marzano, F. Bettio, F. Baccichetti, A. Trevisan, L. Giovagnini, D. Fregona, *Chem. Biol. Interact.* **2004**, *148*, 37–48
- [7] L. Ronconi, C. Marzano, P. Zanello, M. Corsini, G. Miolo, C. Macca, A. Trevisan, D. Fregona, *J. Med. Chem.* **2006**, *49*, 1648–1657
- [8] D. C. Menezes, F. T. Vieira, G. M. de Lima, A. O. Porto, M. E. Cortés, J. D. Ardisson, T. E. Albrecht Schmitt, *Eur. J. Med. Chem.* **2005**, *40*, 1277–1282
- [9] F. A. Allen, *Acta Crystallogr., Sect. B: Struct. Sci.* **2002**, *58*, 380–388
- [10] B. Arul Prakasam, K. Ramalingam, R. Baskaran, G. Bocelli, A. Cantoni, *Polyhedron* **2007**, *26*, 1133–1138
- [11] M. R. L. Oliveira, J. Amim Jr., I. A. Soares, V. M. De Bellis, C. A. de Simone, C. Novais, S. Guillard, *Polyhedron* **2008**, *27*, 727–733
- [12] R. Pastorek, J. Kameníček, J. Husárek, V. Slovák, M. Pavlíček, *J. Coord. Chem.* **2007**, *60*, 485–494
- [13] Z. Trávníček, R. Pastorek, V. Slovák, *Polyhedron* **2008**, *27*, 411–419
- [14] X. Gong, Z. Guo, Z. Wang, *Combust. Flame* **2010**, *157*, 351–356
- [15] Z. H. Wu, L. Xu, Z. Z. Wang, Z. R. Zhang, *Fuel* **2008**, *77*, 891–893
- [16] J. Carrazza, W. T. Tysoc, H. Heinemann, G. A. Somorjai, *J. Catal.* **1985**, *96*, 234–241
- [17] W. J. Lee, S. D. Kim, *Fuel* **1995**, *74*, 1387–1393
- [18] R. Pastorek, J. Kameníček, H. Vrbová, V. Slovák, M. Pavlíček, *J. Coord. Chem.* **2006**, *59*, 437–444

- 1
2 [19] R. Pastorek, J. Kameníček, B. Cvek, V. Slovák, M. Pavlíček,
3 *J. Coord. Chem.* **2006**, *59*, 911–919
4 [20] W. J. Geary, *Coord. Chem. Rev.* **1971**, *7*, 81–122
5 [21] C. A. Tsipis, D. P. Kessissoglou, G. A. Katsoulos, *Chim.*
6 *Chron., New Series* **1985**, *14*, 195
7 [22] S. V. Larionov, L. A. Patrina, I. M. Oglezneva, E. M. Uskov,
8 *Koord. Chim.* **1984**, *10*, 92–99
9 [23] R. P. Scholer, E. A. Merbach, *Inorg. Chim. Acta* **1975**, *15*,
10 15–20
11 [24] L. Ballester, A. Gutierrez, M. F. Perpina, C. Ruiz-Valero,
12 *Polyhedron* **1996**, *15*, 1103–1112
13 [25] A. B. P. Lever in *Inorganic Electronic Spectroscopy (2nd*
14 *edit)*, Elsevier, Amsterdam, **1984**, p. 534
15 [26] C. A. Tsipis, D. P. Kessissoglou, G. E. Manoussakis, *Inorg.*
16 *Chim. Acta* **1982**, *65*, L137–L141
17 [27] C. A. Tsipis, I. E. Meleziadis, D. P. Kessissoglou, G. A.
18 Katsoulos, *Inorg. Chim. Acta* **1984**, *90*, L19–L22
19 [28] D. R. Lide (Ed.) in *Handbook of Chemistry and Physics*
20 *(73rd edit)*, CRC Press, Boca Raton, **1992**
21 [29] F. Březina, E. Benátská, *J. Thermal. Anal.* **1981**, *22*, 75–79
22 [30] Gmelins Handbuch der Anorganischen Chemie, Nickel, Teil
23 C, Lief. 2, Verlag Chemie, GmbH, Weinheim, **1969**, p. 1043
24 [31] G. M. Sheldrick, *Acta Cryst.* **2008**, *A64*, 112–122
25 [32] K. Brandenburg, *DIAMOND, Release 3.1f*, Crystal Impact
26 GbR, Bonn, Germany, **2006**
27 [33] V. Slovák, *Thermochim. Acta* **2001**, *372*, 175–182
28
29
30

31 Received: ((will be filled in by the editorial staff))
32 Published online: ((will be filled in by the editorial staff))
33
34
35
36
37
38
39
40
41
42
43
44
45
46
47
48
49
50
51
52
53
54
55
56
57
58
59
60

Entry for the Table of Contents

Seven nickel(II) *N*-benzyl-*N*-methylthiocarbamate (BzMedtc) complexes were prepared and characterized. The structures of [Ni(BzMedtc)(PPh₃)(NCS)] (**4**) and [Ni(BzMedtc)(PPh₃)₂]ClO₄·H₂O (**5**·H₂O) were determined by a single crystal X-ray analysis, which showed the Ni(II) centre as four-coordinated in a distorted square-planar geometry. The positive catalytic effect of the complexes **1**, **3**, **5**, and **6** on the graphite oxidation was determined. The start temperatures of the oxidation of the complexes were by about 60–100 °C lower in comparison with pure graphite.

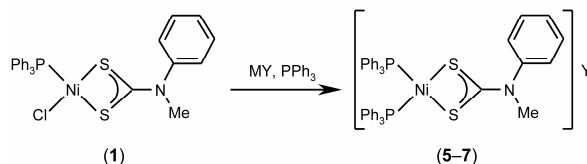


Zdeněk Trávníček,^{*,[a]} Richard Pastorek,^[a] Pavel Štarha,^[a] Igor Popa,^[a] and Václav Slovák^[b]

* Corresponding Author

Fax: +420585 634 357

E-Mail: zdenek.travnicek@upol.cz



X = Cl⁻ (complex **1**), Br⁻ (**2**), I⁻ (**3**), NCS⁻ (**4**)
Y = ClO₄⁻ (**5**), BPh₄⁻ (**6**), PF₆⁻ (**7**)

Nickel(II) *N*-benzyl-*N*-methylthiocarbamate complexes as precursors for the preparation of graphite oxidation accelerators

ARTICLE

DOI: 10.1002/zaac.200

Nickel(II) *N*-benzyl-*N*-methyldithiocarbamate complexes as precursors for the preparation of graphite oxidation accelerators

Zdeněk Trávníček,^{*,[a]} Richard Pastorek,^[a] Pavel Štarha,^[a] Igor Popa,^[a] and Václav Slovák^[b]**Keywords:** Nickel(II) complex; Dithiocarbamate ligand; Crystal structure; Graphite oxidation accelerator.

The nickel(II) *N*-benzyl-*N*-methyldithiocarbamate (BzMedtc) complexes [Ni(BzMedtc)(PPh₃)Cl] (**1**), [Ni(BzMedtc)(PPh₃)Br] (**2**), [Ni(BzMedtc)(PPh₃)I] (**3**) and [Ni(BzMedtc)(PPh₃)(NCS)] (**4**) were synthesized using the reaction of [Ni(BzMedtc)₂] and [NiX₂(PPh₃)₂], where X = Cl, Br, I and NCS. Subsequently, the complex **1** was used for the preparation of [Ni(BzMedtc)(PPh₃)₂]ClO₄ (**5**), [Ni(BzMedtc)(PPh₃)₂]BPh₄ (**6**) and [Ni(BzMedtc)(PPh₃)₂]PF₆ (**7**). The obtained complexes **1–7** were characterized by elemental analysis, thermal analysis and spectroscopic methods (IR, UV-Vis, ³¹P{¹H}-NMR). The results of the magnetochemical and molar conductivity measurements proved the complexes as diamagnetic non-electrolytes (**1–4**) or 1:1 electrolytes (**5–7**).

The molecular structures of **4** and **5**·H₂O were determined by a single crystal X-ray analysis. In all cases, the Ni(II) atom is four-coordinated in a distorted square-planar arrangement with the S₂PX, and S₂P₂ donor set, respectively. The catalytic influence of selected complexes **1**, **3**, **5**, and **6** on graphite oxidation was studied. The results clearly indicated that the presence of the products of thermal degradation processes of the mentioned complexes have impact on the course of graphite oxidation. A decrease in the oxidation start temperatures by about 60–100 °C was observed in the cases of all the tested complexes in comparison with pure graphite.

✉ ^{*} Corresponding Author

Fax: +420585 634 357

E-Mail: zdenek.travnicek@upol.cz

[a] Department of Inorganic Chemistry
Faculty of Science, Palacký University
Tr. 17. listopadu 12, CZ-771 46 Olomouc, Czech Republic

[b] Department of Chemistry
Faculty of Science, University of Ostrava
30. dubna 22, CZ-701 03 Ostrava, Czech Republic
Supporting information for this article is available on the
WWW under <http://dx.doi.org/10.1002/zaac.201000xxx> or
from the author.

Introduction

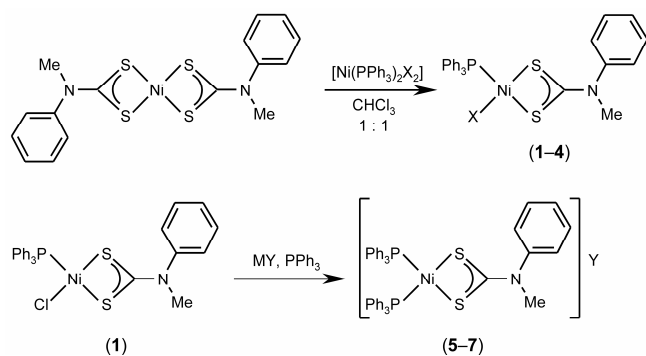
Many compounds involving the dithiocarbamate (dtc) moiety were reported up to now in connection with their applications. These compounds have been found to be useful as fungicides [1] or accelerators of vulcanization [2]. However, the spectrum of potential use of these compounds may be also broadened on the field of *in vitro* anticancer activity as can be demonstrated by the following examples. The 4(3*H*)-quinazolinone derivatives with dithiocarbamate side chains, such as (3,4-dihydro-2-methyl-4-oxoquinazolin-6-yl)-methyl-[4-(4-fluorophenyl)piperazine]-1-carbodithioate, showed promising *in vitro* anticancer activity (IC₅₀ = 0.5 μM) against human myelogenous leukaemia cell line (K562) [3]. Another dithiocarbamate derivative, 4-methylsulfinyl-1-(*S*-methyldithiocarbamyl)-butane (sulforamate), serves as a bearer of cancer chemopreventive effect [4]. The efficient protection of *N*-benzyl-*D*-glucamine-dithiocarbamate against cisplatin-induced nephrotoxicity (it is able to chelate platinum and thus to decrease the possibility of its reactions with sulphur-containing renal proteins or enzymes) has also been reported recently [5].

Several thousands of transition metal complexes involving the dithiocarbamate moiety have been prepared and reported to date and some of them are very promising from the biological activity point of view. The Pt(II) complex of the [Pt(esdt)(py)Cl] composition, where esdt = ethylsarcosinedithiocarbamate and py = pyridine, is highly cytotoxic against several human cancer cell lines, and moreover, this substance was not found as nephrotoxic, contrary to cisplatin [6]. [Au(dmdt)X₂] and [Au(esdt)X₂] are the representatives of non-platinum complex with the promising anticancer activity, which is even higher compared to cisplatin; dmdt = *N,N'*-dimethyldithiocarbamate, X = Cl or Br [7]. The antifungal activity, well-known for dithiocarbamate derivatives, was proved for tin(IV) complexes with pyrrolidine-dithiocarbamate [8].

Nickel is known as a suitable transition metal for the preparation of complexes and it is not surprising that over three thousand compounds (SciFinder, 2010) and 163 X-ray structures (Crystallographic Structural Database, CSD, ver. 5.30, September 2009 update [9]) involving a NiS₂CN motif have been reported to date. Among these compounds, the nickel(II) complexes involving the NiPN(S₂CN) or NiP₂(S₂CN) moiety, such as [Ni(4-MePzdtc)(PPh₃)(NCS)] [10], and [Ni(MeSdtc)(dppe)] [11], respectively, have been described in the literature; 4-MePzdtc = 4-methylpiperazine-dithiocarbamate anion, PPh₃ = triphenylphosphine, MeSdtc = *N*-methyl-*N*-sulfonyldithiocarbamate, dppe = 1,2-bis(diphenylphosphine)ethane. However, no nickel complexes containing the *N*-benzyl-*N*-methyldithiocarbamate anion (BzMedtc) within the mentioned moieties, have been reported to date.

The presented series of compounds follows a great number of nickel dithiocarbamate complexes previously prepared at our department [see ref. 12,13 and the references cited therein]. In this paper, we deal with seven nickel(II) complexes, whose structures, according to the literature research, for the first time involves a combination of the BzMedtc and PPh₃ ligands. The complexes [Ni(BzMedtc)(PPh₃)X] (**1–4**) were synthesized from [Ni(BzMedtc)₂], using its reaction with [NiX₂(PPh₃)₂], where X stands for Cl⁻ (for the complex **1**), Br⁻ (**2**), I⁻ (**3**) and NCS⁻ (**4**). The [Ni(BzMedtc)(PPh₃)₂]Y complexes (Y = ClO₄⁻ for **5**, BPh₄⁻ for **6** and PF₆⁻ for **7**) were prepared by the reaction of complex **1** with the appropriate alkaline salt and triphenylphosphine (see Scheme 1). The products were characterized by various physical methods including ³¹P{¹H}-NMR spectroscopy. The X-ray structures of the representatives of both types of complexes, i.e. [Ni(BzMedtc)(PPh₃)(NCS)] (**4**) and [Ni(BzMedtc)(PPh₃)₂]ClO₄·H₂O (**5**·H₂O), were determined by a single crystal X-ray analysis. The geometry of these compounds is square-planar with the NiS₂PN (**4**) and NiS₂P₂ (**5**·H₂O) donor sets.

This work also describes the effect of the nickel(II) dithiocarbamates on the oxidation of graphite as a model study of the coal combustion. As it is commonly known, the ignition temperature of the coal combustion is one of the most important properties influencing many industrial processes. This stage can be affected by the presence of both natural and artificial impurities [14,15]. Formerly, several papers reported simple nickel(II) compounds, such as NiO (mixed with KOH) or Ni(NO₃)₂ (mixed with K₂SO₄), as the substances accelerating graphite oxidation [16,17]. Few years ago, we decided to study the influence of the nickel(II, IV) dithiocarbamate complexes [see 13,18,19 and references cited therein] on the course of graphite oxidation. It was found that the presence of these complexes causes the ignition temperature decrease. Similar results were obtained also for the tested complexes **1**, **3**, **5**, and **6**, which were chosen as representatives of the presented compounds, as it is discussed in more detail within the framework of this paper.



Scheme 1. Schematic representation of the synthetic procedures applied for the preparation of the nickel(II) complexes **1–7**; X = Cl⁻ (**1**), Br⁻ (**2**), I⁻ (**3**) and NCS⁻ (**4**), MY = LiClO₄·3H₂O (**5**), Na[BPh₄] (**6**) and K[PF₆] (**7**).

Results and Discussion

The nickel(II) complexes **1–7** were prepared according to the synthetic strategies depicted in Scheme 1. The obtained molar conductivity values (Table 1) indicate that complexes **1–4** dissolved in acetone behave as non-electrolytes [20], which indirectly proved the coordination of the Cl⁻ (**1**), Br⁻ (**2**), I⁻ (**3**) and NCS⁻ (**4**) anions to the Ni(II) atom. On the other hand, the molar conductivity values of the remaining complexes proved the ionic nature (1:1 electrolyte type) in acetone (**5**) or DMF (**6**, **7**) solutions, which means that the ClO₄⁻ (**5**), BPh₄⁻ (**6**) and PF₆⁻ (**7**) anions are situated outside of the inner coordination sphere within the structure of the discussed complexes. The results of the room temperature magnetochemical measurements determined the prepared compounds to be diamagnetic, and thus, suggested on square-planar geometries in the vicinity of the central atom.

Table 1: The results of molar conductivity measurements, IR, UV-Vis and ³¹P{¹H}-NMR spectroscopy of the complexes **1–7**

λ_M^a	IR (cm ⁻¹) ^b			UV-Vis (cm ⁻¹) ^c	³¹ P{ ¹ H}-NMR δ^d (ppm)
	$\nu(C\equiv S)$	$\nu(C\equiv N)$	other		
1 2.2	990m	1510m		19 200	21.1s
				25 200	
				29 000	
2 2.1	996m	1520m		18 900	24.8s
				25 000	
				29 000	
3 9.3	998m	1520m		18 400	31.6s
				31 400	
4 1.7	996m	1528m	840m $\nu(C-S)$	20 400	22.8s
			2092s $\nu(C\equiv N)$	29 000	
5 99.0	996w	1542m	622m $\nu_4(ClO_4^-)$	19 900	32.0s
			1088s $\nu_3(ClO_4^-)$	31 000	
6 77.3	990m	1536s		20 700	32.1s
				30 900	
7 66.9	996m	1540m	836m $\nu_4(PF_6^-)$	19 800	32.0s,
				29 300	-143.6sp

[a] S cm² mol⁻¹ (10⁻³ M acetone solutions for **1–5** and 5 × 10⁻⁴ M DMF solutions for **6** and **7**); [b] KBr pellets (w = weak, m = middle, s = strong); [c] nujol technique; [d] CDCl₃ solutions (s = singlet, sp = septuplet)

Spectroscopic Characterization

The PPh₃ signals in the ³¹P{¹H}-NMR spectra of the CDCl₃ solutions of **1–7** were found in the range of 21.1–32.1 ppm (Table 1). These values differ significantly from that of -4.52 ppm determined for the free PPh₃ molecule, which is caused by electron density redistribution from phosphorus towards the Ni(II) centre as a consequence of PPh₃ coordination. The spectrum of **7** contains a septuplet at -143.6 ppm assignable to the PF₆⁻ anion. It should be noted that the chemical shift values of the complexes **1–4** increased in the order [Ni(Cl)(BzMedtc)(PPh₃)] (**1**) < [Ni(NCS)(BzMedtc)(PPh₃)] (**4**) < [Ni(Br)(BzMedtc)(PPh₃)] (**2**) < [Ni(I)(BzMedtc)(PPh₃)] (**3**), which agrees with the results reported for the nickel(II) complexes with *N*-benzyl-*N*-butyldithiocarbamate [12].

The maxima observed in the IR spectra of the nickel(II) complexes **1–7** at 990–998 cm⁻¹, and 1510–1542 cm⁻¹ (see Table 1) are typical for the $\nu(C\equiv S)$, and $\nu(C\equiv N)$ vibrations of the dithiocarbamate moiety, respectively [21,22]. The

peak of the $\nu(\text{C}=\text{S})$ stretching vibration is not split, which supports the bidentate coordination of the BzMedtc anion. The peaks of the $\nu(\text{C}\equiv\text{N})$ and $\nu(\text{C}-\text{S})$ vibrations of the NCS^- anion were observed in the IR spectrum of **4**. The ionic nature of the perchlorate anion in the complex **5**, can be supported by two undivided peaks at 622 and 1088 cm^{-1} [23]. The same conclusion can be made for the complex **7**, whose IR spectrum contains the non-split peak at 836 cm^{-1} assignable to $\nu(\text{PF}_6^-)$, which again indicates its ionic nature [24].

Table 2. Crystal data and structure refinements for $[\text{Ni}(\text{NCS})(\text{BzMedtc})(\text{PPh}_3)]$ (**4**) and $[\text{Ni}(\text{BzMedtc})(\text{PPh}_3)_2]\text{ClO}_4\cdot\text{H}_2\text{O}$ (**5**· H_2O)

Compound	4	5 · H_2O
Empirical formula	$\text{C}_{28}\text{H}_{25}\text{N}_2\text{NiPS}_3$	$\text{C}_{45}\text{H}_{42}\text{ClNNiO}_5\text{P}_2\text{S}_2$
Formula weight	575.36	897.02
Temperature (K)	113(2)	110(2)
Wavelength (\AA)	0.71073	0.71073
Crystal system	Monoclinic	Triclinic
Space group	$P2_1/n$	$P-1$
a (\AA)	13.6177(3)	11.47995(13)
b (\AA)	10.3556(2)	13.24049(16)
c (\AA)	19.1287(4)	15.02884(19)
α ($^\circ$)	90	70.3319(11)
β ($^\circ$)	92.4015(18)	84.5683(10)
γ ($^\circ$)	90	87.3995(9)
V (\AA^3)	2695.6(9)	2141.23(4)
Z , D_{calc} (g cm^{-3})	4, 1.418	2, 1.391
Absorption coefficient	1.032 mm^{-1}	0.734 mm^{-1}
Crystal size (mm)	0.30×0.25×0.25	0.40×0.35×0.30
$F(000)$	1192	932
θ range for data collection ($^\circ$)	$2.90 \leq \theta \leq 25.00$	$3.03 \leq \theta \leq 25.00$
Index ranges (h, k, l)	$-16 \leq h \leq 16$ $-9 \leq k \leq 12$ $-22 \leq l \leq 22$	$-13 \leq h \leq 13$ $-15 \leq k \leq 15$ $-17 \leq l \leq 15$
Reflections collected/unique	22656/4743	18531/7526
(R_{int})	(0.0246)	(0.0108)
Max./min. transmission	0.7825/0.7471	0.8099/0.7578
Data/restraints/parameters	4743/0/317	7526/0/553
Goodness-of-fit on F^2	1.065	1.039
Final R indices [$I > 2\sigma(I)$]	$R_1 = 0.0282$, $wR_2 = 0.0673$	$R_1 = 0.0342$, $wR_2 = 0.1009$
R indices (all data)	$R_1 = 0.0366$, $wR_2 = 0.0692$	$R_1 = 0.0388$, $wR_2 = 0.1031$
Largest peak/hole (e \AA^{-3})	0.344/−0.212	1.343 and −0.611

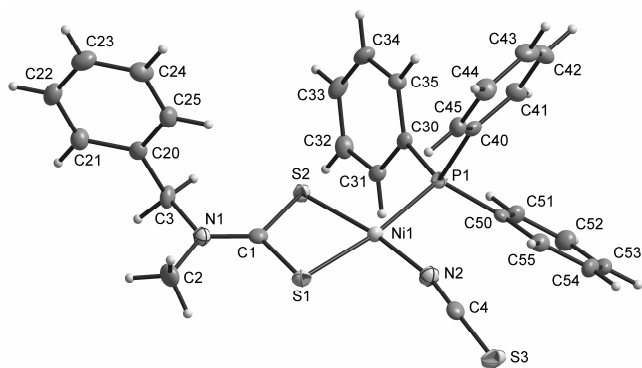


Figure 1. The molecular structure of $[\text{Ni}(\text{BzMedtc})(\text{PPh}_3)(\text{NCS})]$ complex (**4**) with non-hydrogen atoms drawn as thermal ellipsoids at the 50% probability level.

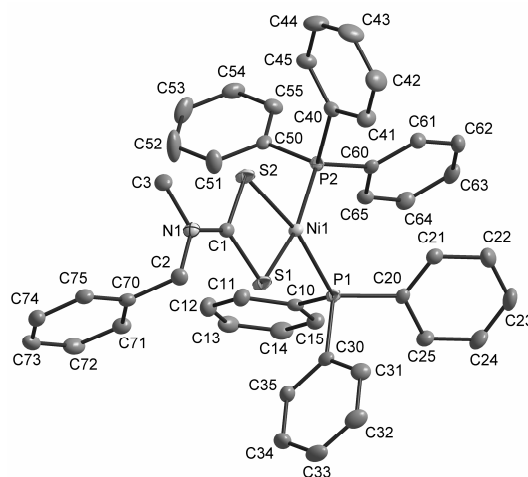


Figure 2. The molecular structure of $[\text{Ni}(\text{BzMedtc})(\text{PPh}_3)_2]\text{ClO}_4\cdot\text{H}_2\text{O}$ (**5**· H_2O) with non-hydrogen atoms drawn as thermal ellipsoids at the 50% probability level. The hydrogen atoms, perchlorate anion and water molecule of crystallization were omitted for clarity.

Diffuse-reflectance electronic spectra of the prepared complexes **1–7** support the assumption of the square-planar geometry in the vicinity of the central Ni(II) atom. Absorption maxima at the 18 400–20 700 cm^{-1} region may be attributed to the $^1A_{1g} \rightarrow ^1B_{1g}$ transition of the square-planar nickel(II) complexes [25,26]. The next maxima, also assignable to the $d-d$ transitions, were found for the complexes **1** (25 200 cm^{-1}) and **2** (25 000 cm^{-1}). The maxima above 29 000 cm^{-1} are probably connected with the intraligand charge-transfer transitions in the S_2CN moiety [27].

X-ray Structure of $[\text{Ni}(\text{NCS})(\text{BzMedtc})(\text{PPh}_3)]$ (**4**) and $[\text{Ni}(\text{BzMedtc})(\text{PPh}_3)_2]\text{ClO}_4\cdot\text{H}_2\text{O}$ (**5**· H_2O)

The X-ray structure of the title complexes **4** (Figure 1) and **5**· H_2O (Figure 2) was determined by a single crystal X-ray analysis. The crystal data and structure refinements are given in Table 2, while the selected bond lengths and angles are summarized in Table 3.

The central Ni(II) ion of the complex **4** (Figure 1) is four-coordinated by PPh_3 , the isothiocyanate anion, and the bidentate-coordinated N -benzyl- N -methyldithiocarbamate anion (BzMedtc). The atoms of a NiS_2NP chromophore are arranged in the distorted square-planar geometry around the metal centre (Table 3). The Ni–S bond lengths of the title complex correlate well with the mean value of 2.204 \AA (2.155–2.258 \AA interval) determined for this band for the 116 square-planar nickel complexes involving bidentate-coordinated dithiocarbamate S-donor ligands, which have been up to now deposited in the Cambridge Structural Database (CSD) [9].

The well-known delocalization of π -electron density within the S_2CN moiety of the dithiocarbamate anion was observed for **4**, since the C–N and C–S bond lengths of the

studied compound (Table 2) were found to be significantly shorter compared to the single C–N (1.47 Å) and C–S (1.81 Å) σ -bond lengths [28]. Further, the C–S and C–N bond length values of BzMedtc are comparable with those of the transition metal (TM) complexes involving the (TM) S_2CNR_2 moiety and deposited within the CSD, which equal 1.717 Å, and 1.326 Å, respectively.

The S1 atom is the most deviated one [0.0454(5) Å] from the plane created through the Ni1, S1, S2, P1 and N2 atoms of the chromophore. Further, the described plane forms the dihedral angle of 83.10(5)° with the benzene ring of the BzMedtc anion and dihedral angles of 67.90(5)°, 69.63(5)° and 47.85(4)° with the benzene rings of PPh₃ containing the C30, C40, and C50 atoms, respectively. Mutual orientation of the phenyl groups of PPh₃ within the molecular structure of **4** can be described by the 67.64(6)° (between benzene rings containing C30 and C40), 66.06(6)° (between benzene rings containing C30 and C50) and 76.53(6)° (between benzene rings containing C40 and C50) dihedral angles. The C–H...C, C–H...S and C...C types of the intermolecular non-bonding van der Waals contacts were detected to stabilize the crystal structure of **4** (see Table 4). No typical hydrogen bond is present within the structure of discussed complex.

Table 3: Selected bond lengths (Å) and angles (°) for the complexes [Ni(NCS)(BzMedtc)(PPh₃)] (**4**) and [Ni(BzMedtc)(PPh₃)₂]ClO₄·H₂O (**5**·H₂O)

Compound	4	5 ·H ₂ O
<i>Bond Lengths</i>		
Ni1–S1	2.2245(5)	2.2154(6)
Ni1–S2	2.1758(5)	2.2257(6)
Ni1–P1	2.2162(5)	2.2165(6)
Ni1–P2	-	2.2316(6)
Ni1–N2	1.8564(17)	-
C1–S1	1.7125(19)	1.731(2)
C1–S2	1.7214(19)	1.721(2)
C1–N1	1.306(2)	1.307(3)
N2–C4	1.163(2)	-
C4–S3	1.621(2)	-
<i>Bond Angles</i>		
S1–Ni1–S2	78.643(19)	78.29(2)
S1–Ni1–P1	171.63(2)	91.28(2)
S1–Ni1–N2	92.06(5)	-
S1–Ni1–P2	-	167.08(2)
S2–Ni1–P1	93.384(19)	167.76(2)
S2–Ni1–P2	-	88.91(2)
S2–Ni1–N2	170.70(5)	-
P1–Ni1–N2	95.91(5)	-
P1–Ni1–P2	-	101.24(2)
Ni1–S1–C1	85.71(7)	86.52(8)
Ni1–S2–C1	87.04(7)	86.42(8)
S1–C1–S2	108.60(11)	108.61(12)
S1–C1–N1	125.67(15)	126.50(17)
S2–C1–N1	125.73(15)	124.89(17)
Ni1–N2–C4	167.29(16)	-
N2–C4–S3	178.52(19)	-

In the case of **5**·H₂O, the Ni(II) ion is four-coordinated in the distorted square-planar geometry (Figure 2), similarly to the above described structure of complex **4**, by the bidentate-coordinated S-donor BzMedtc ligand and by two P-donor PPh₃ molecules. Selected bond lengths and angles

are given in Table 3. The positive charge of the [Ni(BzMedtc)(PPh₃)₂]⁺ cation is compensated by the perchlorate anion; the shortest Ni1...Cl1 distance equals 7.131(2) Å.

Table 4 Selected intermolecular non-bonding contacts and their parameters (Å, °) determined for the complexes **4** and **5**·H₂O

D–H...A	<i>d</i> (D–H)	<i>d</i> (H...A)	<i>d</i> (D...A)	<(DHA)
4				
C3–H3A...S3 ⁱ	0.990	2.9234(6)	3.666(2)	132.43(12)
C34–H34A...S2 ⁱⁱ	0.950	2.9389(5)	3.717(2)	139.90(12)
C32–H32A...S3 ⁱⁱⁱ	0.950	2.8695(6)	3.814(2)	172.48(12)
C31–H31A...S1 ⁱⁱⁱ	0.950	2.9701(6)	3.883(2)	161.56(12)
C2...C32			3.307(3)	
5 ·H ₂ O				
C74–H74A...C32 ^{iv}	0.950	2.771(3)	3.678(4)	160.13(16)
C72–H72A...C54 ^v	0.950	2.781(2)	3.554(3)	139.11(16)
C2–H2B...C74 ^{iv}	0.990	2.844(2)	3.771(3)	156.25(14)
C14–H14A...C33 ^{vi}	0.950	2.746(3)	3.666(4)	163.31(16)
C13–H13A...C3 ^v	0.950	2.879(2)	3.815(3)	168.16(14)
C44–H44A...C64 ^{vii}	0.950	2.872(3)	3.653(4)	140.17(16)
C13...C71 ^v			3.262(4)	
C70...C70 ^{iv}			3.391(3)	

Symmetry codes: (i) $x + 0.5, 0.5 - y, z - 0.5$; (ii) $1 - x, 1 - y, 1 - z$; (iii) $1.5 - x, y + 0.5, 1.5 - z$; (iv) $-x, -y, -z$; (v) $-x, 1 - y, -z$; (vi) $1 - x, 1 - y, -z$; (vii) $-x, 1 - y, 1 - z$

As it has been already mentioned in the case of complex **4**, the bond lengths within the NiS₂CN moiety of both structures show on electron density redistribution in connection with π -electron density delocalization (see the C–S and C–N bond lengths in Table 3). As for the Ni–P bonds of **5**, their lengths are in good agreement with the mean value of 2.208 Å (2.175–2.252 Å interval) as determined from 36 X-ray structures of tetra-coordinated nickel dithiocarbamate complexes involving at least one PPh₃ ligand and deposited within the CSD.

The S2 atom is the most deviated one [0.0903(6) Å] from the plane created through the atoms of the chromophore. The dihedral angles between this plane and benzene rings involving C10, C20, C30, C40, C50, C60, and C70 are 86.39(5)°, 58.49(7)°, 87.97(5)°, 70.52(5)°, 71.64(5)°, 63.60(6)°, and 71.98(5)°, respectively. Non-bonding interactions of the C–H...C and C...C types (C–H...O interactions with the distorted perchlorate anion and water molecule of crystallization are disregarded) were found in the crystal structure of the discussed nickel(II) complex (Table 4).

TG/DTA Thermal Analysis

The thermal properties of the prepared nickel(II) complexes were studied by TG and DTA methods. The TG and DTA curves of **1** and **6** are depicted in Figure 3. Although the chemical composition of these complexes is different, their thermal decomposition proceeded in a similar manner as indicated by analogical shapes of the TG curves. In cases of **2**, **3** and **6**, the sharp *exo*-effects with maxima at 188 °C, 193 °C, and 188 °C, respectively, were accompanied by mass increase on the TG curves, which can be attributed to the oxygen atom insertion into the Ni–P bond [29]. This effect was not registered on the TG curves of the remaining complexes, where the oxygen atom

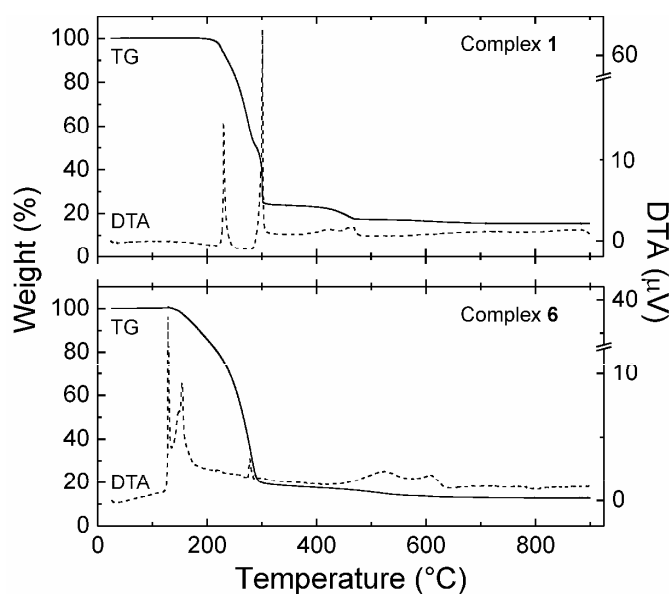


Figure 3. TG/DTA curves for complexes 1 and 6.

insertion is most likely combined with the decomposition of the organic parts of the studied complexes.

The final products of the TG studies (900 °C) were studied by X-ray powder diffraction (XRD). NiO (PDF-4 No. 01-089-7130) was determined as the final product of the thermal decomposition of 1–4. In the cases of the complexes 6 and 7, the mixtures with significant predominance of NiO were detected. The final product of the TG thermal study of 6 also contains NiS (PDF-4 No. 4-004-5027) and Ni₃B₂O₆ (PDF-4 No. 4-008-3203), and some peaks could not be assigned. As for the complex 7, Ni₂P₂O₇ (PDF-4 No. 01-074-1604) and Ni₃(PO₄)₂ (PDF-4 No. 01-072-3977) were detected by a XRD, while some peaks were not assigned.

Catalytic Influence of the Complexes on Graphite Oxidation

The influence of the presence of the representative complexes 1, 3, 5 and 6 on graphite oxidation were studied. The results, summarized in Figure 4 (obtained DTG curves) and Table 5 (obtained data), showed an positive influence on graphite oxidation, because the ignition temperature significantly decreased (by about 64–99 °C) after the addition of the tested nickel(II) complexes to a pure graphite.

Pure graphite oxidation proceeds in one step, while in the cases of its mixtures with the tested complexes, two steps in a larger temperature interval were detected on the appropriate DTG curves (Table 5). The first step takes place at lower temperature than pure graphite oxidation, whereas the oxidation rate maxima (T_m) of the second step approximately correspond to pure graphite. In addition, the oxidation mechanisms of both steps are different, as it can be seen from the activation energy (E) and frequency factor (A) values given in Table 5. More graphite was oxidized during the second step with higher E and A values.

At this point, we would like to discuss the described results of the influence on the graphite oxidation in connection with the results of TG/DTA studies. Figure 3 clearly shows that the thermal decomposition of the nickel(II) complexes is almost completely finished at the temperature of ca. 700 °C and the weight loss above this temperature is insignificant. Based on this statement it may be concluded that not directly the discussed nickel(II) *N*-benzyl-*N*-methyldithiocarbamate complexes, but the products of their thermal decomposition processes, affected graphite oxidation.

Table 5: Characteristic temperatures and kinetic parameters of catalytic influence on graphite given for pure graphite and its mixtures with nickel(II) complexes 1, 3, 5 and 6

Sample	T (°C)	T_m (°C)	Step	n	A (s ⁻¹)	E	w (%)
Graphite	778–859	832		0.7	1.97×10^9	247	
1	679–838	792	I	1.3	3.62×10^7	190	43.58
			II	0.9	1.09×10^9	235	56.42
3	696–879	838	I	0.9	4.08×10^6	174	34.48
			II	0.9	9.10×10^7	220	65.52
5	693–860	815	I	1.0	1.47×10^7	183	36.06
			II	1.0	4.08×10^9	250	63.94
6	714–861	812	I	0.8	5.88×10^6	176	23.48
			II	1.1	1.17×10^9	238	76.52

T = temperature range of oxidation; T_m = oxidation rate maximum; n = reaction order; A = frequency factor; E = activation energy (kJ mol⁻¹); w = mass of sample oxidized

In connection with the above-mentioned facts, the tested complexes (except of 5) were heated *in situ* to the temperatures corresponding to the beginning and end of graphite oxidation (see Table 5). The products of thermal decomposition relating to the mentioned temperatures were analysed by XRD. As for 1–4, pure NiO was identified at both temperatures (Figure 5). The slight differences in the 2θ values were caused by a dilatation of the sample due to different measurement temperature. On the other hand, the mixtures of NiO, NiS and Ni₃B₂O₆ (for 6) and Ni₂P₂O₇ and

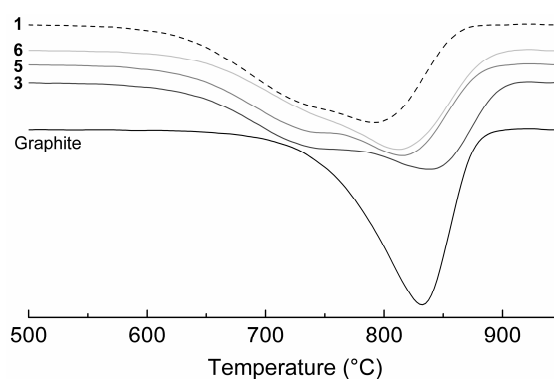


Figure 4. DTG curves obtained for pure graphite (black lines) and its mixture with the complexes 1 (black dashed lines), 3 (dark gray line), 5 (gray line) and 6 (light gray line); the tangent method was employed to determine the initial temperatures of the graphite oxidation

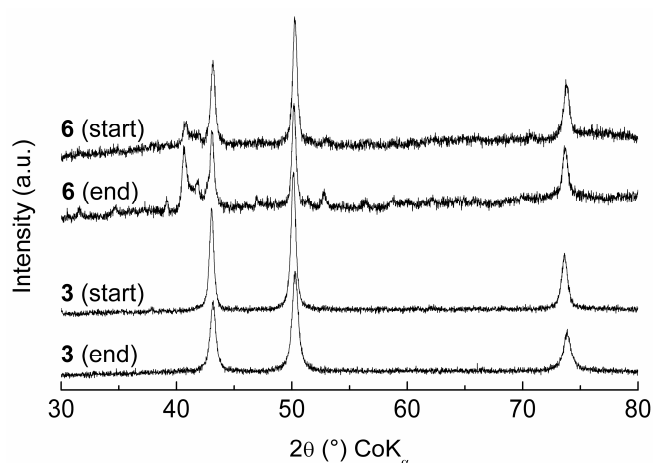


Figure 5. XRD patterns of the thermal decomposition products of the complexes **3** and **6**. The detected diffraction lines belong to NiO for **3**, and NiO, NiS and Ni₃B₂O₆ for **6**; the start and end temperatures are given in Table 5.

Ni₃(PO₄)₂ (for **7**) were detected by an XRD (Figure 5). Their quantitative composition was similar at both temperatures. Some peaks could not be assigned again.

Conclusions

Seven nickel(II) complexes of the [Ni(BzMedtc)(PPh₃)X] (**1–4**) and [Ni(BzMedtc)(PPh₃)₂]Y (**5–7**) compositions were synthesized; X = Cl⁻ for **1**, Br⁻ for **2**, I⁻ for **3** and NCS⁻ for **4**, Y = ClO₄⁻ for **5**, BPh₄⁻ for **6** and PF₆⁻ for **7**). The obtained powder products were fully characterized by elemental analysis, magnetochemical and molar conductivity measurements, thermal analysis and spectroscopic methods (IR, UV-Vis, ³¹P{¹H}-NMR). The molecular structures of the complexes [Ni(BzMedtc)(PPh₃)(NCS)] (**4**) and [Ni(BzMedtc)(PPh₃)₂]ClO₄·H₂O (**5**·H₂O) were determined by a single crystal X-ray analysis, which proved the distorted square-planar geometry with the bidentate-coordinated S-donor BzMedtc anion accompanied by PPh₃ and NCS⁻ (**4**) or by two PPh₃ (**5**). This paper also describes the significant catalytic influence of the thermal degradation products of the selected complexes **1**, **3**, **5**, and **6** on graphite oxidation.

Experimental Section

Materials and General Methods

Chemicals and solvents were purchased from Sigma-Aldrich Co., Acros Organics Co., Lachema Co. and Fluka Co. and they were used as received. The starting compounds [Ni(BzMedtc)₂], [Ni(PPh₃)₂Cl₂], [Ni(PPh₃)₂Br₂], [Ni(PPh₃)₂I₂] and [Ni(PPh₃)₂(NCS)₂] were prepared according to the formerly reported synthetic pathways [13,30].

Elemental analyses (C, H, N) were performed on a Fisons EA-1108 CHNS-O Elemental Analyzer (Thermo Scientific). The content of nickel was determined using the chelatometric titration with murexide as an indicator. Chlorine, bromine and iodine contents were determined by the Schöniger method. Diffuse-reflectance spectra were recorded on a Perkin-Elmer Lambda35 UV/Vis

spectrometer using a nujol technique. IR spectra (KBr pellets) were recorded on a Perkin-Elmer Spectrum one FT-IR spectrometer in the 450–4000 cm⁻¹ region. The molar conductivity values of 10⁻³ M acetone solutions of **1–5** and 5 × 10⁻⁴ M *N,N'*-dimethylformamide (DMF) solutions of **6** and **7** were determined by an LF 330/SET conductometer (WTW GmbH) at 25 °C. The room temperature magnetic susceptibilities were measured using the Faraday method with a laboratory designed instrument with a Sartorius 4434 MP-8 microbalance; Co[Hg(NCS)₄] was used as a calibrant and the correction for diamagnetism was performed using Pascal constants. Simultaneous thermogravimetric (TG) and differential thermal (DTA) analyses were performed by an Exstar TG/DTA 6200 (Seiko Instruments Inc.) in a platinum crucible and dynamic air atmosphere (100 mL min⁻¹) from the laboratory temperature to 1050 °C with a 2.5 °C min⁻¹ temperature gradient. The weights of the studied complexes **1–4**, **6** and **7** (**5** was not studied for safety reasons, since it contains the perchlorate anion) were ca. 10 mg. ³¹P{¹H}-NMR spectra of the CDCl₃ solutions were measured on a Bruker Avance 300 spectrometer at 300 K and the spectra were calibrated against 85% H₃PO₄ used as an external reference. X-ray powder diffraction experiments were performed with a PANalytical X'Pert PRO instrument (Co-K_α radiation) equipped with an X'Celerator detector. Samples were placed on a zero-background Si slide and scanned in the 2θ range of 5–90° in the steps of 0.017°. *In situ* measurements were realized in the reaction cell XRK900 (Anton Paar). Evaluation was made using HighScore Plus software and PDF-4 database.

Single Crystal X-ray Analysis of the Complexes **4** and **5**·H₂O

A single crystal X-ray measurement was performed on an XcaliburTM2 diffractometer (Oxford Diffraction Ltd.) with Sapphire2 CCD detector, and with Mo K_α (Monochromator Enhance, Oxford Diffraction Ltd.) and at 113 K (**4**) and 110 K (**5**·H₂O). Data collection and reduction were performed by a CrysAlis software [CrysAlis CCD and CrysAlis RED, Version 1.171.33.52, Oxford Diffraction Ltd., Abingdon, England, 2009]. The same software was used for data correction for an absorption effect by the empirical absorption correction using spherical harmonics, implemented in SCALE3 ABSPACK scaling algorithm. Both structures were solved by direct methods using SHELXS-97 software [31] and refined on *F*² using the full-matrix least-squares procedure (SHELXL-97). Non-hydrogen atoms were refined anisotropically and all hydrogen atoms were located in difference Fourier maps and refined by using the riding model with C–H = 0.95, 0.98 and 0.99 Å, and *U*_{iso}(H) = 1.2*U*_{eq}(CH, CH₂) or 1.5*U*_{eq}(CH₃), except for those belonging to the crystal water molecule in **5**. The perchlorate anion as well as crystal water molecule was refined as disordered over two positions with the occupancy factors 75% and 25%, and 57% and 43%, respectively. The crystal data and structure refinements of **4** and **5** are given in Table 1. The molecular graphics were drawn and the additional structural calculations were interpreted using DIAMOND [32]. Crystallographic data have been deposited with the Cambridge Crystallographic Data Centre, 12 Union Road, Cambridge CB21EZ, UK (Fax: +44-1223-336033; E-Mail: deposit@ccdc.cam.ac.uk). Copies of the data can be obtained free of charge on application to CCDC, as the depository numbers CCDC-766048 (**4**) and CCDC-766049 (**5**·H₂O).

The Catalytic Study

Graphite (0.6 g, diameter of particles less than 0.1 mm, ash residue max. 0.2%, mass drying loss max. 0.2%) was mixed with an acetone solution (2 mL) of the nickel(II) complex **1**, **3**, **5** or **6** (**2**, **4**, and **7** were not studied because of their insufficient solubility in acetone) to give the final nickel concentration of 2.5 mmol L⁻¹. The mixtures were homogenized and dried at room temperature for 24 h. The study of the catalytic influence of these samples on graphite was performed on a Netzsch STA 449C device with an α -Al₂O₃ crucible without a standard (10 °C min⁻¹ heating rate, sample weight of 5.0 mg, 100 mL min⁻¹ dynamic air atmosphere). The intersection point of the DTG curve tangents represents the initial temperatures of the graphite oxidation. The kinetic parameters were calculated by a direct non-linear regression method [33].

Syntheses of the Nickel(II) Complexes 1–7

[Ni(BzMedtc)(PPh₃)Cl] (1), **[Ni(BzMedtc)(PPh₃)Br] (2)**, **[Ni(BzMedtc)(PPh₃)] (3)** and **[Ni(BzMedtc)(PPh₃)(NCS)] (4)**: The complex **1** was synthesized using the reaction of [Ni(BzMedtc)₂] (1 mmol) and [NiCl₂(PPh₃)₂] (1 mmol). Both starting compounds were suspended in 25 mL of chloroform (CHCl₃). The mixture was stirred at room temperature until the reaction components were completely dissolved. The resulting solution was filtered through activated carbon. Diethyl ether was added to the filtrate which was left to stand at laboratory temperature. The precipitate of **1** formed in a few days. The product was filtered off, washed with diethyl ether and dried at 40 °C under an infrared lamp. The complexes **2–4** were prepared as described for **1**, but [NiBr₂(PPh₃)₂] (for **2**), [NiI₂(PPh₃)₂] (for **3**) and [Ni(NCS)₂(PPh₃)₂] (for **4**) were used instead of [NiCl₂(PPh₃)₂]. In the case of the complex **4**, the crystals suitable for a single crystal X-ray analysis were obtained from the mother liquor in two days. **[Ni(BzMedtc)(PPh₃)Cl] (1)**: Yield: 78%. Colour: violet. C₂₇H₂₅NS₂PClNi (M_r = 552.8); C 58.7 (calc. 58.4); H 4.6 (4.6); N 2.5 (2.4); S 11.6 (11.3); Cl 6.4 (6.5); Ni 10.6 (10.6)%. TG/DTA data: the decomposition began at 177 °C and finished at 704 °C with the experimental weight loss of 84.5% (calc. to NiO residue: 86.5%), exothermic peaks with the maxima at 231, 302, 420 and 463 °C.

[Ni(BzMedtc)(PPh₃)Br] (2): Yield: 90%. Colour: violet. C₂₇H₂₅NS₂PBrNi (M_r = 597.2); C 54.3 (calc. 54.2); H 4.2 (4.1); N 2.3 (2.0); S 10.7 (10.3); Br 13.4 (13.1); Ni 9.8 (9.6)%. TG/DTA data: the decomposition began at 156 °C and finished at 1000 °C with the weight loss of 86.0% (calc. to NiO residue: 87.5%), exothermic peaks with the maxima at 188, 282, 398 and 490 °C.

[Ni(BzMedtc)(PPh₃)] (3): Yield: 70%. Colour: dark violet. C₂₇H₂₅NS₂PINi (M_r = 644.2); C 50.3 (calc. 49.9); H 3.9 (3.9); N 2.2 (2.2); S 10.0 (10.0); I 19.7 (19.3); Ni 9.1 (9.2)%. TG/DTA data: the decomposition began at 180 °C and finished at 829 °C with the weight loss of 86.6% (calc. to NiO residue: 88.4%), endothermic peak with the maximum at 269 °C and exothermic peaks with the maxima at 193, 246, 301, 457 and 544 °C.

[Ni(BzMedtc)(PPh₃)(NCS)] (4): Yield: 82%. Colour: red. C₂₈H₂₅N₂S₃PNi (M_r = 575.4); C 58.5 (calc. 58.9); H 4.4 (4.1); N 4.9 (4.7); S 16.7 (16.6); Ni 10.2 (10.3)%. TG/DTA data: the decomposition began at 155 °C and finished at 1047 °C with the weight loss of 84.7% (calc. to NiO residue: 87.0%), endothermic peak with the maximum at 198 °C and exothermic peaks with the maxima at 227, 304, 336, 442 and 541 °C.

[Ni(BzMedtc)(PPh₃)₂]ClO₄ (5): LiClO₄·3H₂O (2 mmol) was poured to a suspension of the complex **1** (1 mmol) and PPh₃ (2 mmol) in methanol (25 mL). The reaction mixtures were refluxed for 3 h. The resulting solution was filtered through activated carbon and left to stand at room temperature. The crystals of **5**·H₂O suitable for a single crystal X-ray analysis formed from the mother liquor in a few days. The complex was filtered off, washed with methanol and diethyl ether and dried at 40 °C under an infrared lamp. Yield: 47%. Colour: pink. C₄₅H₄₀NS₂P₂ClO₄Ni (M_r = 879.0); C 61.5 (calc. 61.8); H 4.6 (4.3); N 1.6 (1.5); S 7.3 (6.9); Cl 4.2 (4.6); Ni 6.7 (6.8)%.

[Ni(BzMedtc)(PPh₃)₂]BPh₄ (6): 2 mmol of Na[BPh₄] was added to a suspension of **1** (1 mmol) and PPh₃ (2 mmol) in 25 mL of methanol. The pink solid appeared during 3 h of the reaction mixture refluxing. The product was removed by filtration, washed (methanol and diethyl ether) and dried at 40 °C under an infrared lamp. Yield: 69%. Colour: pink. C₆₉H₆₀NS₂P₂BNi (M_r = 1098.8); C 75.4 (calc. 75.1); H 5.5 (5.2); N 1.3 (1.5); S 5.8 (5.6); Ni 5.3 (5.7)%. TG/DTA data: the decomposition began at 124 °C and finished at 764 °C, exothermic peaks with the maxima at 128, 154, 178, 524 and 607 °C.

[Ni(BzMedtc)(PPh₃)₂]PF₆ (7): The solutions of PPh₃ (2 mmol; 5 mL of acetone) and K[PF₆] (1 mmol; 7 mL of acetone) were separately added to a solution of **1** (1 mmol; 5 mL of chloroform). The reaction mixture was refluxed for a period of 4 h and after that it was filtered through activated carbon. Diethyl ether was added to the filtrate, which caused the formation of the precipitate. The solid was filtered off, washed with diethyl ether and dried at 40 °C under an infrared lamp. Yield: 54%. Colour: red. C₄₅H₄₀NS₂P₃F₆Ni (M_r = 924.5); C 58.5 (calc. 58.8); H 4.4 (4.6); N 1.6 (1.9); S 6.9 (6.5); Ni 6.3 (6.7)%. TG/DTA data: the decomposition began at 99 °C and finished at 782 °C, exothermic peaks with the maxima at 188, 207, 310 and 472 °C.

Acknowledgement

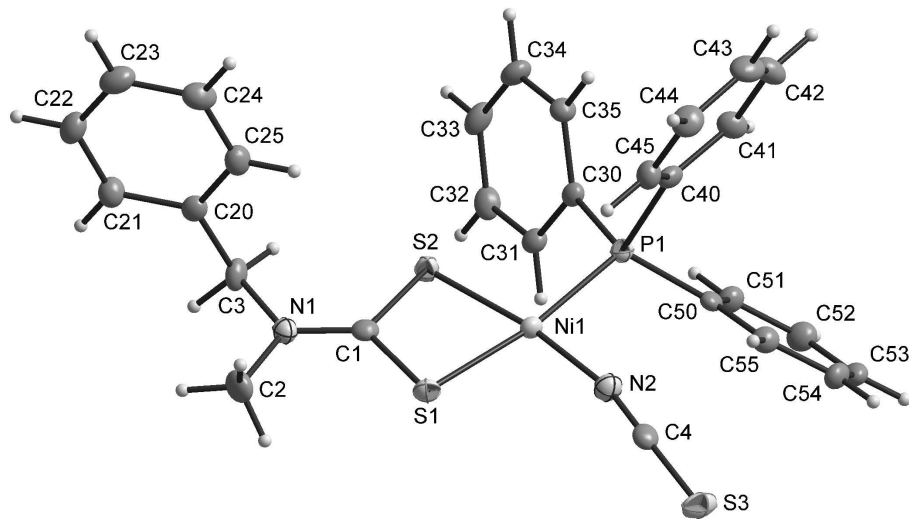
This work was financially supported by The Ministry of Education, Youth and Sports of the Czech Republic (a grant no. MSM6198959218). The authors also thank Assoc. Prof. Zdeněk Šindelář for magnetic susceptibility measurements, and Dr. Jan Filip for X-Ray powder diffraction experiments.

References

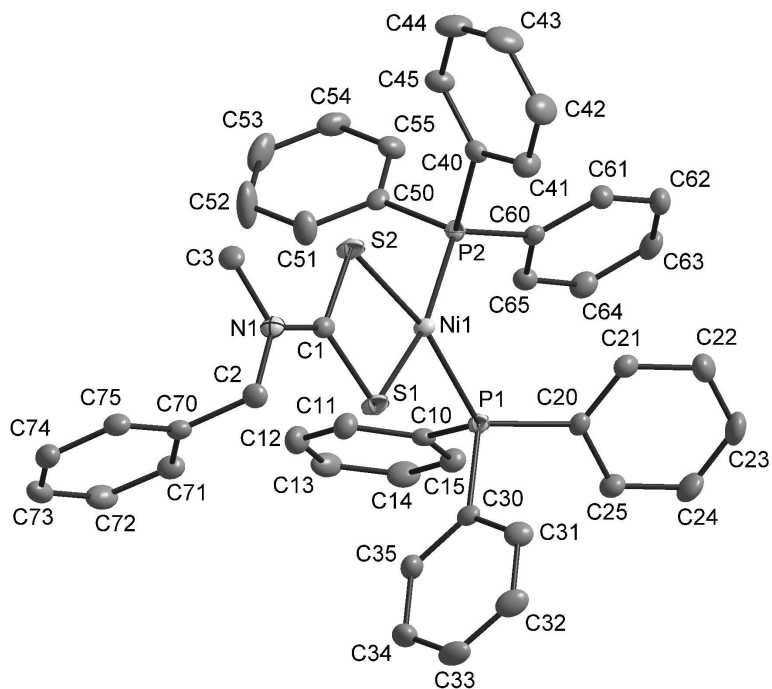
- [1] G. Hogarth, *Prog. Inorg. Chem.* **2005**, *53*, 71–561
- [2] P. J. Nieuwenhuizen, A. W. Ehlers, J. G. Haasnoot, S. R. Janse, J. Reedijk, E. J. Baerends, *J. Am. Chem. Soc.* **1999**, *121*, 163–168
- [3] S. L. Cao, Y. P. Feng, Y. Y. Jiang, S. Y. Liu, G. Y. Ding, R. T. Li, *Bioorg. Med. Chem.* **2005**, *15*, 1915–1917
- [4] C. Gerhauser, M. You, J. Liu, R. M. Moriarty, M. Hawthorne, R. G. Metha, R. C. Moon, J. M. Pezzuto, *Cancer Res.* **1997**, *57*, 272–278
- [5] S. Hidaka, T. Funakoshi, H. Shimada, M. Tsuruoka, S. Kojima, *J. App. Toxicol.* **1995**, *15*, 167–273
- [6] C. Marzano, F. Bettio, F. Baccichetti, A. Trevisan, L. Giovagnini, D. Fregona, *Chem. Biol. Interact.* **2004**, *148*, 37–48
- [7] L. Ronconi, C. Marzano, P. Zanello, M. Corsini, G. Miolo, C. Macca, A. Trevisan, D. Fregona, *J. Med. Chem.* **2006**, *49*, 1648–1657

- 1
2 [8] D. C. Menezes, F. T. Vieira, G. M. de Lima, A. O. Porto, M.
3 E. Cortés, J. D. Ardisson, T. E. Albrecht Schmitt, *Eur. J.*
4 *Med. Chem.* **2005**, *40*, 1277–1282
- 5 [9] F. A. Allen, *Acta Crystallogr., Sect. B: Struct. Sci.* **2002**, *58*,
6 380–388
- 7 [10] B. Arul Prakasam, K. Ramalingam, R. Baskaran, G. Bocelli,
8 A. Cantoni, *Polyhedron* **2007**, *26*, 1133–1138
- 9 [11] M. R. L. Oliveira, J. Amim Jr., I. A. Soares, V. M. De Bellis,
10 C. A. de Simone, C. Novais, S. Guilardi, *Polyhedron* **2008**,
11 *27*, 727–733
- 12 [12] R. Pastorek, J. Kameníček, J. Husárek, V. Slovák, M.
13 Pavlíček, *J. Coord. Chem.* **2007**, *60*, 485–494
- 14 [13] Z. Trávníček, R. Pastorek, V. Slovák, *Polyhedron* **2008**, *27*,
15 411–419
- 16 [14] X. Gong, Z. Guo, Z. Wang, *Combust. Flame* **2010**, *157*, 351–
17 356
- 18 [15] Z. H. Wu, L. Xu, Z. Z. Wang, Z. R. Zhang, *Fuel* **2008**, *77*,
19 891–893
- 20 [16] J. Carrazza, W. T. Tysoe, H. Heinemann, G. A. Somorjai, *J.*
21 *Catal.* **1985**, *96*, 234–241
- 22 [17] W. J. Lee, S. D. Kim, *Fuel* **1995**, *74*, 1387–1393
- 23 [18] R. Pastorek, J. Kameníček, H. Vrbová, V. Slovák, M.
24 Pavlíček, *J. Coord. Chem.* **2006**, *59*, 437–444
- 25 [19] R. Pastorek, J. Kameníček, B. Cvek, V. Slovák, M. Pavlíček,
26 *J. Coord. Chem.* **2006**, *59*, 911–919
- 27 [20] W. J. Geary, *Coord. Chem. Rev.* **1971**, *7*, 81–122
- 28 [21] C. A. Tsipis, D. P. Kessissoglou, G. A. Katsoulos, *Chim.*
29 *Chron., New Series* **1985**, *14*, 195
- 30 [22] S. V. Larionov, L. A. Patrina, I. M. Oglezneva, E. M. Uskov,
31 *Koord. Chim.* **1984**, *10*, 92–99
- 32 [23] R. P. Scholer, E. A. Merbach, *Inorg. Chim. Acta* **1975**, *15*,
33 15–20
- 34 [24] L. Ballester, A. Gutierrez, M. F. Perpnan, C. Ruiz-Valero,
35 *Polyhedron* **1996**, *15*, 1103–1112
- 36 [25] A. B. P. Lever in *Inorganic Electronic Spectroscopy (2nd*
37 *edit)*, Elsevier, Amsterdam, **1984**, p. 534
- 38 [26] C. A. Tsipis, D. P. Kessissoglou, G. E. Manoussakis, *Inorg.*
39 *Chim. Acta* **1982**, *65*, L137–L141
- 40 [27] C. A. Tsipis, I. E. Meleziadis, D. P. Kessissoglou, G. A.
41 Katsoulos, *Inorg. Chim. Acta* **1984**, *90*, L19–L22
- 42 [28] D. R. Lide (Ed.) in *Handbook of Chemistry and Physics*
43 *(73rd edit)*, CRC Press, Boca Raton, **1992**
- 44 [29] F. Březina, E. Benátská, *J. Thermal. Anal.* **1981**, *22*, 75–79
- 45 [30] Gmelins Handbuch der Anorganischen Chemie, Nickel, Teil
46 C, Lief. 2, Verlag Chemie, GmbH, Weinheim, **1969**, p. 1043
- 47 [31] G. M. Sheldrick, *Acta Cryst.* **2008**, *A64*, 112–122
- 48 [32] K. Brandenburg, *DIAMOND, Release 3.1f*, Crystal Impact
49 GbR, Bonn, Germany, **2006**
- 50 [33] V. Slovák, *Thermochim. Acta* **2001**, *372*, 175–182
- 51
52
53
54

55 Received: ((will be filled in by the editorial staff))
56 Published online: ((will be filled in by the editorial staff))
57
58
59
60

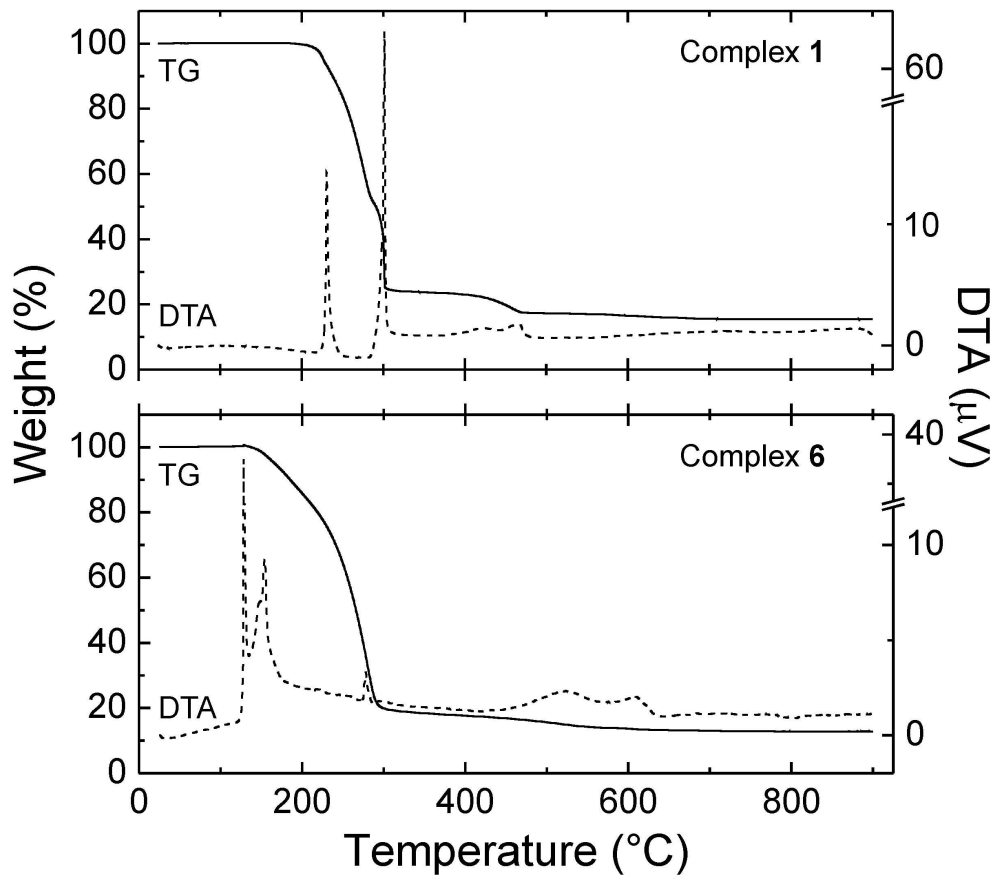


The molecular structure of $[\text{Ni}(\text{BzMedtc})(\text{PPh}_3)(\text{NCS})]$ complex (4) with non hydrogen atoms drawn as thermal ellipsoids at the 50% probability level.
1216x926mm (96 x 96 DPI)



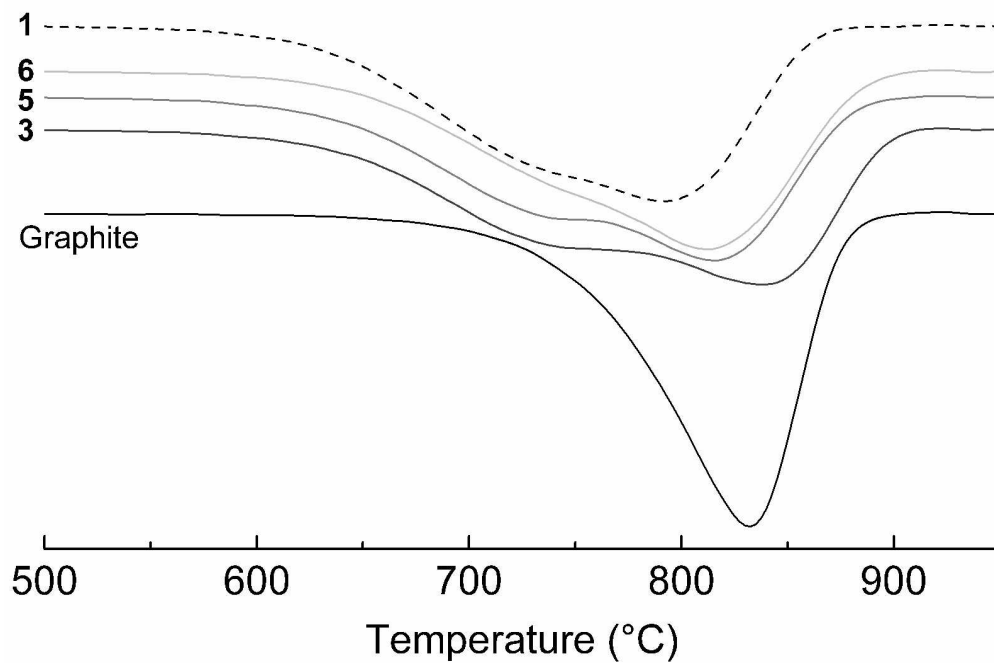
The molecular structure of $[\text{Ni}(\text{BzMedtc})(\text{PPh}_3)_2]\text{ClO}_4 \cdot \text{H}_2\text{O}$ ($5 \cdot \text{H}_2\text{O}$) with non hydrogen atoms drawn as thermal ellipsoids at the 50% probability level. The hydrogen atoms, perchlorate anion and water molecule of crystallization were omitted for clarity.

1216x926mm (96 x 96 DPI)

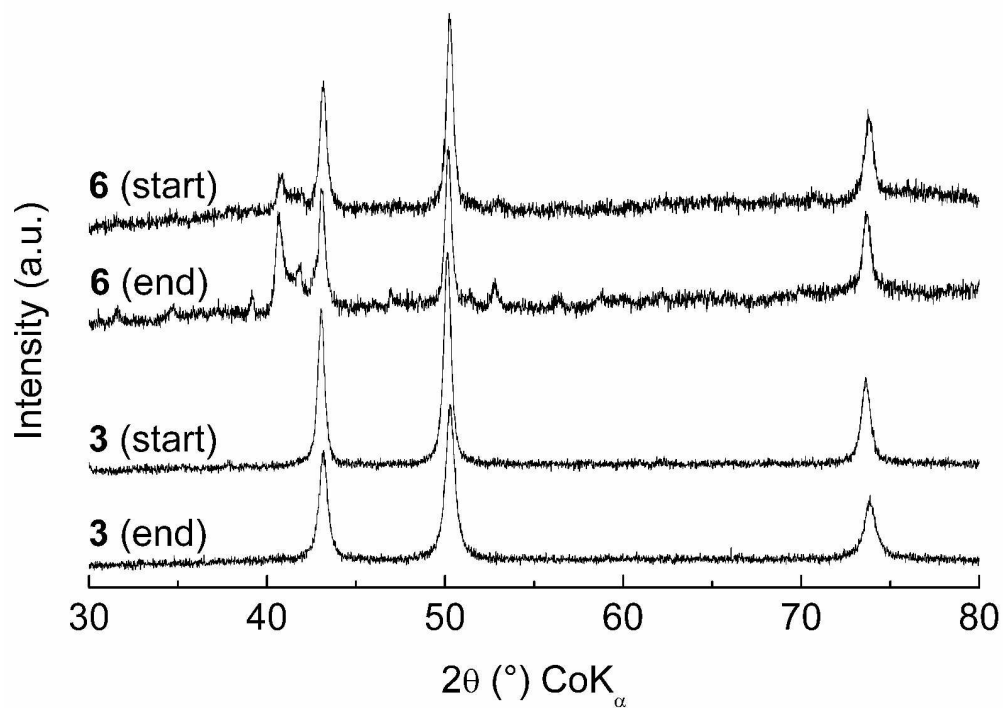


TG/DTA curves for complexes 1 and 6.
103x90mm (600 x 600 DPI)

1
2
3
4
5
6
7
8
9
10
11
12
13
14
15
16
17
18
19
20
21
22
23
24
25
26
27
28
29
30
31
32
33
34
35
36
37
38
39
40
41
42
43
44
45
46
47
48
49
50
51
52
53
54
55
56
57
58
59
60

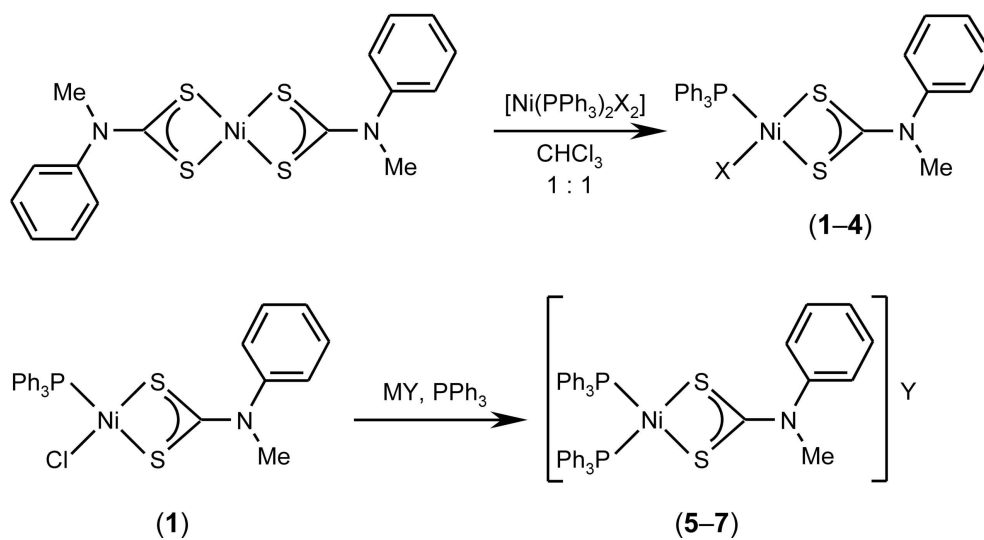


DTG curves obtained for pure graphite (black lines) and its mixture with the complexes 1 (black dashed lines), 3 (dark gray line), 5 (gray line) and 6 (light gray line); the tangent method was employed to determine the initial temperatures of the graphite oxidation
269x192mm (600 x 600 DPI)



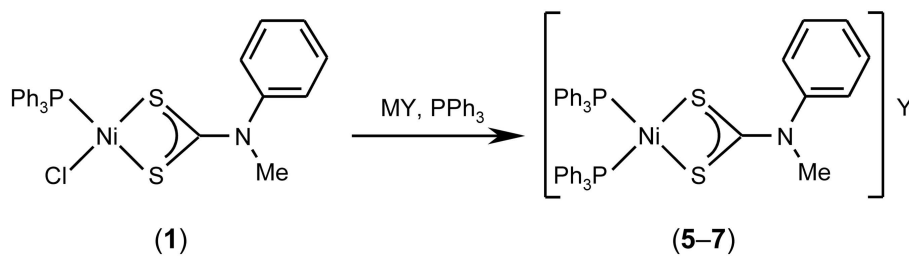
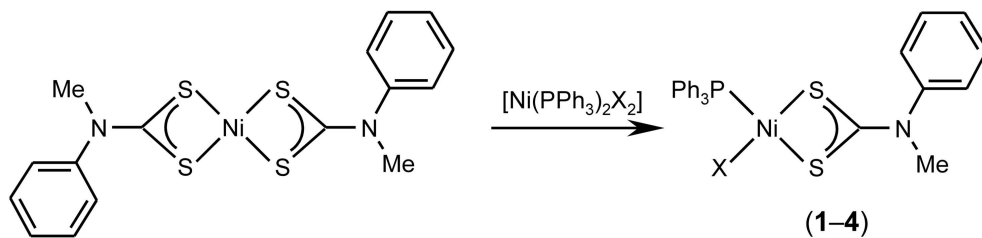
XRD patterns of the thermal decomposition products of the complexes 3 and 6. The detected diffraction lines belong to NiO for 3, and NiO, NiS and Ni₃B₂O₆ for 6; the start and end temperatures are given in Table 5.

269x192mm (600 x 600 DPI)



Schematic representation of the synthetic procedures applied for the preparation of the nickel(II) complexes 1-7; X = Cl⁻ (1), Br⁻ (2), I⁻ (3) and NCS⁻ (4), MY = LiClO₄•3H₂O (5), Na[BPh₄] (6) and K[PF₆] (7).

109x58mm (600 x 600 DPI)



26 X = Cl⁻ (complex **1**), Br⁻ (**2**), I⁻ (**3**), NCS⁻ (**4**)

27 Y = ClO₄⁻ (**5**), BPh₄⁻ (**6**), PF₆⁻ (**7**)

28
29 Table of Contents Graphic
30 125x76mm (600 x 600 DPI)